LARS Information Note 110873

An Analysis of Temporal Data for Crop Species Classification and Urban Change Detection

P. Anuta
M. Bauer

The Laboratory for Applications of Remote Sensing

Purdue University, West Lafayette, Indiana

1973

LARS Information Note: 110873

An Analysis of Temporal Data for Crop Species Classification and Urban Change Detection

Paul E. Anuta and Marvin E. Bauer

Laboratory for Applications of Remote Sensing
Purdue University
West Lafayette, Indiana

I. Introduction

Machine analysis of remote sensor imagery from aircraft and satellite sensors has primarily utilized the spectral measurement dimension [1, 2, 3, 4, 17]. In spectral analysis, the scene is examined in terms of its reflectivity or emissivity. The spectral measurements are essentially instantaneous in time for each scene element. Two other forms of measurements can be made in conjunction with the measurement of reflected energy. The shape or spatial structure of scene objects can be observed and utilized to aid in extracting information from the measurements. Such analysis implies an imaging sensor which measures energy in a two-dimensional format with received energy being spatially resolvable to some given level. The second form is measurement of temporal variations and refers to the observation of reflected or

---

The work described in this report was sponsored by the National Aeronautics & Space Administration (NASA) under Grant Number NGL-15-005-112 and Contract No. NAS-5-21773.

radiated energy as a function of time. The measurements can represent total energy in a broad portion of the spectrum or can be detailed spectral analysis of the instantaneous energy received as a function of time.

Utilization of spatial structure in remote sensor imagery requires effective feature extraction procedures to derive size, shape, and textural characteristics from observed scenes, and this problem is among the most challenging in the pattern recognition field [5]. Observation of time or temporal variations on the other hand requires only that the basic spectral measurement be repeated continuously or at discrete intervals.

The key consideration to be made in considering the implementation of a particular measurement scheme is that of the effectiveness of the resulting data in solving a particular problem. Spectral measurements have proven particularly effective in the recognition of crop species and other natural features [17]. Spatial measurements are necessary for character recognition and detection of objects having distinct shape. Temporal variations are basic to the transmission of sound and information through communication channels. The use of temporal data in the context of remote sensing is relatively new. Interest is growing in the area of automatic change detection via temporal images [6, 7] and crop species

detection has been explored using temporal variations in photographic brightness as a measurement vector [8]. In the work reported here the use of temporal variations in the multispectral scanner imagery from the NASA Earth Resources Technology Satellite (ERTS-1) is explored for crop recognition and urban and agricultural feature change detection.

Observation of changes in energy in one or several spectral bands for points in an image can be carried out manually; however, the concern of this study is machine (computer) implementation of the information extraction processes. Numerical observation of changes in the energy received from image elements requires that each element be stored in geometrical coincidence such that all such elements can be addressed by a single coordinate pair and a spectral/temporal independent variable [9]. Achieving coincidence is known as image registration and must be achieved before computer analysis of temporal data can take place. The image registration problem will be discussed in general and then a specific solution implementation will be described in Section II. The output of the registration phase is a digital multi-image with N spectral/temporal channels. For example, if four spectral bands and four times are represented, the multi-image will contain 16 channels. Registered ERTS-1 images are assumed to be an input to this study.

ERTS-1 multispectral scanner data from two areas are analyzed. The first is an agricultural area near DeKalb in Northern Illinois and the other is the Lafayette Area in North Central Indiana. Data from ERTS-1 frames covering these areas were spatially registered to produce a multi-channel spectral/temporal data set for each area. Section II describes the test data sets and the analysis algorithms which were used. Section III describes the use of pattern recognition techniques to classify data from a test site in Northern Illinois using spectral and temporal data. Section IV describes a method and presents test results for detecting change in agricultural and urban scenes using multispectral change data. Section V contains a summary and conclusions.

II. Data Description and Analysis Techniques

ERTS Data Bands

Spectral measurements of reflected energy by ERTS-1 are confined to the .5 to 1.1 micrometer portion of the electromagnetic spectrum [10]. This region is split into four bands and the energy in each is measured and recorded for discrete points in the image viewed. The earth surface area covered by each measurement is assumed to be a square of 79 meters on a side. Thus, the spectral multi-image consists of vectors of four elements each containing energy measurements in the following bands:

Channel	
1	.5 - .6 micrometers (green)
2	.6 - .7 micrometers (red)
3	.7 - .8 micrometers (infrared)
4	.8 - 1.1 micrometers (infrared)

An example of an ERTS-1 image set is presented in Figure 1. The area represented is approximately 26 by 27 miles and the image consists of 403,200 discrete numerical energy values converted to a gray scale level and presented on a cathode ray tube screen [11].

Spatial data is not used in the evaluation performed here, thus spectral response values are independent of their relative position in the image. Let $X_{ij}^{k}(t)$ by the numerical value representing the image sample at row i, column j, from channel k

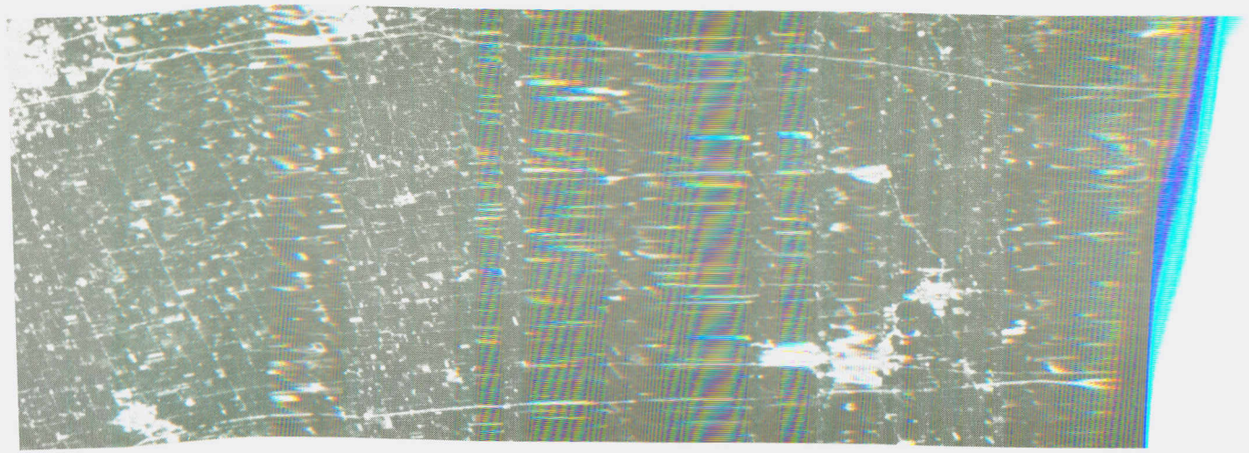

.5-.6 micrometer band

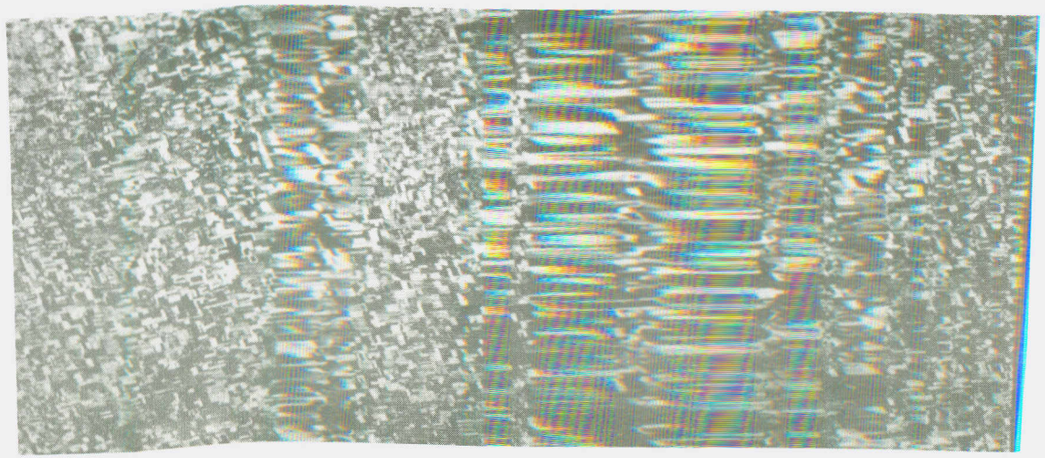

.7-.8 micrometer band

Figure 1. Example of ERTS-1 multispectral imagery of Salt Lake City in the vicinity of the Great Salt Lake, Utah, August 9, 1972.

at time t. The sample value is a positive integer having a maximum value of 127, i.e., 7 binary digits. A set of registered multispectral images obtained at times t_1, t_2....t_N of the same area form a multispectral/multitemporal hyper-image in a four dimensional coordinate system. The multi-image is thus defined by an integer variable and four parameters:

$$X^k_{ij}(t_\ell) = \text{Array of Image Points}$$

with:

$k=1,...,NC$ = Number of Channels
$i=1,...,NRW$ = Number of Rows
$j=1,...,NCO$ = Number of Columns
$\ell=1,...,NT$ = Number of Times

and for the ERTS-1 system X is integer with $0 \leq X \leq 127$

Information Extraction

A basic distinction is made here between the concepts of "image processing" and "information processing". Image processing is generally thought of as referring to enhancement, error correction, coding, etc. of images to increase their value to human observers without the process of information extraction necessarily being included in the machine processing phase. Information processing on the other hand endeavors to derive a measure of information from the input data. In general, the information measure will be a real number

defining some quantity of interest to a user. This output quantity can represent scene cover type, i.e. corn, soybeans, house, road, water, etc. or some more abstract measure. The desire here is to introduce the concept of the Information Functional to describe all processes of reducing measurement vectors or functions to a number or perhaps a number which points to a set of numbers which represent useful information to interested parties.

Information Functionals

Given a Multispectral, Multitemporal or other measurement space M we wish to model or reduce M to an information quantity. Define the information functional L(X) as a linear or nonlinear transformation of elements of M (all $X \varepsilon M$) into an information space S which will in this work be the field of positive integers or real numbers. For example, a multispectral response function $X(\lambda)$ or $X(\lambda,t)$ consisting of measurements from an agricultural scene is transformed into an integer denoting a class such as corn or soybeans by a classification algorithm. In LARSYS [1] the information functional C=L(X) (where X is the multispectral function of wavelength $X(\lambda)$, C is the class decision and L is the classifier function) takes the form of the maximum likelihood ratio algorithm:

$$L(X) = \left[X \rightarrow C ; \max_{C} \left[P(X|\omega_C) P(\omega_C) \right] \right]$$

Where: $P(X|\omega_c)$ is the probability density function for class c.

$P(\omega_c)$ is the a priori probability of class c.

Any transformation from a measurement space into an information space will be called an information functional. The concept generalizes the process of data analysis and prevents excessive attention from being placed on any one classification process.

Relationship of Spectral and Temporal Dimensions

The new channels added by the repeated coverage of the same area can be treated as additional spectral channels and used in the same way as the spectral channels. Thus, the temporal dimension is absorbed into the set of measurements for each image point and thought of as part of a general measurement space. Pattern classification techniques can then be applied to the expanded measurement space and the benefits of the added channels can be evaluated using existing multispectral analysis techniques. This is the approach followed in the first part of this work. The set of multispectral images is treated as an NxP channel multi-image (N channels and P times) and a crop classification experiment is conducted using the combined data set.

The repeated coverage of a scene can also be treated as a new measurement form and special processing structures can

be developed for dealing with the new form of data. This is the approach followed in the second part of the work reported here. The interest was in detecting significant changes in the scene from one time to another. The change detection work is thus restricted to the analysis of only two images gathered at two different times. The object is to detect the location and nature of significant changes between the two times using the multispectral images obtained at each of the two times. A change detection scheme is proposed here which uses the multi-dimensional pattern recognition technique with pattern classes "change" and "no change" defined rather than "corn", "soybeans", etc.

Spatial Registration of Time Sequential ERTS Frames

Registration of multiple images of the same scene was accomplished through use of the LARS image registration system which is described in [9]. The overlay processing operation consists of two basic operations: 1.) image correlation and 2.) overlay transformation which are performed sequentially. Many factors exist which prevent exact overlay of the images, thus this operation is approximate. Two major errors are: (1) It is unlikely that the samples from one time were imaged from exactly the same spot as samples from a later satellite pass, thus, in general, no data exists which exactly overlays for both times even if no other errors were present; and (2) Due to changes in the scene and other "noise" sources the two

images cannot be exactly correlated or matched. The overlay procedure used consists of the following:

1. Initial checkpoints or matching points are manually selected in the two images to be overlayed using the LARS digital display [11]. At least seven points are found and the coordinates are recorded on punched cards. Each checkpoint consists of an ordered quadruple of coordinates:

$$P = (X_A^{(k)}, Y_A^{(k)}, X_B^{(k)}, Y_B^{(k)})$$

with X_A, Y_A being the coordinate of a point in the A or reference image and X_B, Y_B being the coordinates of the corresponding point in the B image to be overlayed on the A image. This step in essence removes rotational misalignment and reduces translational misregistration to 10 to 20 pixels.

2. A two dimensional least squares quadratic polynomial is generated to represent the difference in position of points in the A and B images. The polynomial is of the form:

$$\Delta X = a_0 + a_1 x + a_2 y + a_3 x^2 + a_4 y^2 + a_5 xy$$

$$\Delta Y = b_0 + b_k x + b_2 y + b_3 x^2 + b_4 y^2 + b_5 xy$$

and the least squares solution for the coefficients is:

$$\underline{\alpha} = (P^T P)^{-1} P^T \delta_x$$

$$\underline{\beta} = (P^T P)^{-1} P^T \delta_y$$

Where: α,β are 6x1 coefficient vectors for $\Delta X\&Y$, P is the matrix $[P_{ij}]$ of powers of X and Y for each checkpoint: $P_{ij} = X_i^k Y_i^\ell$ where i is the number of the checkpoint, i=1,N;k= 0,1,0,2,0,1; ℓ = 0,0,1,0,2,1 for j= 1,2,3,4,5,6 respectively.

$\delta_{x,y}$= Nx1 column vector of differences between A and B coordinates, $\delta_{x_i} = X_{B_i} - X_{A_i}$, $\delta_{y_i} = Y_{B_i} - Y_{A_i}$

This function describes an approximate overlay of A and B.

3. A block image cross correlator is employed to find the remaining image displacement at the nodes of a uniform grid using the approximate overlay polynomial generated in (2). The correlator implements the correlation coefficient equation:

$$R(k,\ell) = \frac{E[(A - M_A)\ (B_{k,\ell} - M_B)]}{\sqrt{E[(A - M_A)^2]E[(B_{k,\ell} - M_B)^2]}}$$

Where E denotes mathematical expectation, $M_{A,B}$ the mean values of A and B data blocks and the k,ℓ subscript on B denotes the shift of the B block with respect to the A block of k rows and ℓ columns. As large a set of correlations as possible is obtained within computation time constraints. The k,ℓ values at the maximum R are

chosen as the correct shift to match the block from image B to the block from image A. This peak is interpolated using 3 point LaGrange polynomials to produce a fractional estimate of shift. The set of shifts from the correlator are added to the shift values from the original polynomial to form a new set of checkpoints.

4. A new overlay polynomial is generated from the correlator produced set of checkpoints and used to actually overlay the images. The nearest neighbor rule is employed to obtain points where no data exists. The A and B images are combined onto one data tape and a new data set is formed having M+N channels where M is the number of channels from image A and N is the number of channels from image B.

5. The overlay data tape is inspected to check image quality and overlay quality. Precise evaluation of overlay accuracy is not possible. A measure of error is obtained from the residual from the least squares polynomial generation operation and this figure averages .5 of an image sample, RMS. The two areas analyzed in this study were processed in this manner and the multispectral/ multitemporal data tapes thus generated were used as input. Further discussion of registration techniques is outside the scope of this paper.

Geometric Transformation

For certain applications geometric correction of the ERTS MSS data is desirable. Although the ERTS photographic products obtained from NASA have been geometrically corrected for scale, skew, and other errors the digital data used for computer analysis is not corrected. Thus, when the digital data is reproduced in image form on a line printer or CRT device all the system geometric errors are present. For applications such as urban change detection precise location of each pixel is required so that single pixel phenomena can be ground checked. An existing geometric correction process was applied to the data used in the change detection study (Part IV) to approximately geometrically correct the ERTS data. The resulting data when printed on a computer line printer in pictorial form has a scale of 1" = 24000" and is physically overlayable on USGS topographic maps of the same scale. Thus, individual pixels could be located on the map for accurate ground observation. The details of the correction are not given here but are available in a LARS report [12].

Multidimensional Image Classification Methods

Two multidimensional image analysis methods were used in the study [13]. A non-supervised or clustering procedure was employed to find initial separable classes or groups of points in the data over small areas. The results of the non-supervised

analysis are used directly and for defining training areas for the second analysis method: supervised classification. Supervised classification requires specification of parameters for each class to be recognized and this method can generally handle larger areas than the non-supervised approach and hopefully produces higher accuracy due to its use of second order statistics. These two methods are described briefly below.

Non-Supervised Analysis Method

The clustering procedure [14] used is one of many possible implementations and this particular algorithm uses an iterative process in which all vectors are assigned to current cluster centers using Euclidian distance and linear decision boundaries. The mean vectors of the resulting clusters are computed and these form the new cluster centers. The process is repeated until no vectors change cluster from one step to another. The clustering process can be precisely stated in the following manner. Let S be the set of all data vectors to be clustered into m clusters. The desired set of clusters is the partition $P^*=\{P_1,P_2,..P_m\}$ of S which covers S and for which some metric D(P) for the partitions is minimum. (i.e., $U_{i=1}^{m}P_i=S$ and $\bigcap_{i=1}^{m}P_i=\emptyset$). For the clustering procedure used here $D(P)=\sum_{i=1}^{m}|P_i-\bar{P}_i|$ where $\bar{P}_i$ is the mean or cluster center of cluster P_i and $|P_i-\bar{P}_i|$

denotes the Euclidian distances from $\bar{P}_i$ to each point in P_i. The resulting information functional is a mapping from measurement functions into cluster numbers: $C=NS(x(\lambda,t))$ where x is the function of wavelength (λ) and time (t) and $C= 1,2,...m$, m being the total number of clusters found in the data set.

There are two parameters to be specified as input to the clustering process: 1.) Number of clusters to be found and 2.) Number of channels to be used. Both choices have only a weak basis in theory and heuristic methods are generally used on a trial and error basis. The number of clusters chosen to be found depends largely on how many possible categories of interest exist in the data. This is the heuristic aspect of cluster number selection. A measure of cluster separation is obtained by computing a higher order metric or norm for the final cluster relationships. A measure called the distance quotient [13] or Swain-Fu distance is used. The Swain-Fu distance is a measure of the pairwise separation between cluster centers:

$$Q= \frac{D_{12}}{D_1+D_2}$$

Where: D_{12}= Euclidian distance between cluster centers

D_1 = Distance from cluster center 1 to "edge"* of cluster 1 along line to cluster center 2.

D_2 = Same for cluster 2 with respect to cluster 1.

Since Q is a pairwise measure there are $m = \frac{n!}{2(n-2)!}$ Q's for n clusters. The average quotient for all m pairs, $\bar{Q}$, is a measure of overall cluster separation and could be used to compare results using different numbers of clusters. Increasing $\bar{Q}$'s indicate increasing average separation between clusters.

The heuristic method of cluster number selection tends to be dominant since the numerical measures do not always agree with the desired real world result. In the case of change detection two or three clusters might be desired: 1.) Change and 2.) No change; or 1.) Change type 1, 2.) Change type 2, and 3.) No change. The meaning of Q can be depicted by two circles, Figure 2, representing cluster 1 and cluster 2. A value of 1 for Q indicates that the clusters are just touching, whereas a value of .75 indicates an overlap of 50% and a Q of 1.5 indicates total separation. Thus an average Q of 1 or more would indicate separable or distinct clusters. Use of this measure will be described in the application examples which follow.

---

* See reference 13 for definition of edge.

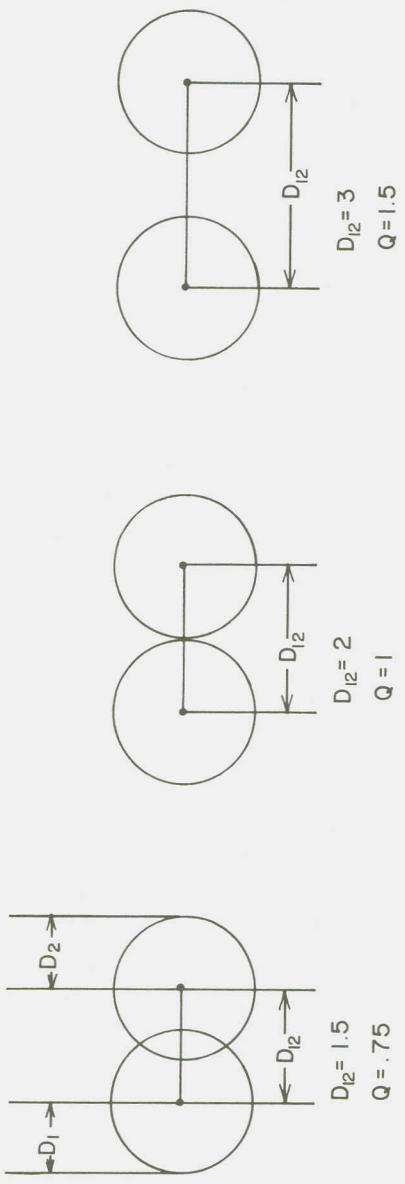

Figure 2. Cluster Separation Geometry assuming $D_1=D_2=1$ and circular distributions.

Supervised Classification

In supervised classification the cluster output is inspected and groups of points are selected which represent categories of interest. To do this, the cluster map is overlayed on topographic maps or aerial photographs having the same scale so that the surface features of interest in the imagery can be identified. The sets of points representing these materials are then used as training for the classifier. The information functional form here is $C=SC(X|T)$ where X is the measurement function, T is the set of training parameters and C is the class decision.

The supervised pattern recognition system used to compare the data forms was developed at LARS and consists of several processors for statistical analysis, classification, and display of digital multi-image data. This system, referred to as LARSYS, is described in [1] and [13] and elsewhere. It is sufficient to point out here that maximum likelihood ratio classification is performed using training statistics based on the assumption that the data is multivariate normal, or Gaussian, distributed. Training and test samples are selected from the test site data and used to train and test the classification of all points in the area (the training and test sets are independent).

Test Sites and Dates of Coverage

The test sites for the study were in Northern Illinois near DeKalb and in Tippecanoe County in North Central Indiana. The dates of the ERTS-1 data coverage for the two test areas are:

TIME	NORTHERN ILLINOIS	NORTH CENTRAL INDIANA
1	August 9, 1972	September 30, 1972
2	September 19, 1972	October 19, 1972
3	October 2, 1972	November 24, 1972
4	———	June 9, 1973

III. Crop Classification Using Temporal Data

The first approach to using temporal data was to add the new measurements obtained at time $t_2, t_3, \ldots$ to those obtained at time t_1 and utilize the expanded feature space. The three time ERTS spectral/temporal data set discussed above offers twelve dimensions for analysis. All or any subset of these dimensions, or channels as they will be called, can be used to recognize objects or cover types in the scene. As part of an ERTS-1 data evaluation project, extensive analysis has been performed at LARS on ERTS-1 data from the Northern Illinois test site using purely spectral measurements from the August 9, 1972 overpass [17].

The primary cover types in the area are corn and soybeans with minor classes of wheat, oats, sorghum, urban, roads, etc. Corn and soybeans cover approximately 60% of the surface in this area. Classification results using pure spectral data are compared with results using mixed spectral and temporal data as the method of evaluation of the temporal dimension. Purely spectral channels were used first to determine the results obtainable without temporal data. The training and test samples were classified using the spectral channels from August 9, September 19 and October 2 in separate experiments.

One facility of the LARSYS system is a feature selection

algorithm [15] which computes the optimum subset of a given set of channels for separating a set of classes. The feature selection processor chooses the channel set which gives the best overall separability; however, individual classes may not all increase in classification accuracy as the number of channels used is increased. This processor was used to select the best single, two, and three channels from the four available from the ERTS MSS data. These channels were used to classify the training and test samples using the procedures described above. The results are presented in Table 1a thru f.

It is seen that in most of the cases the overall classification accuracy increases with increasing dimension; however, addition of channel one adds relatively little or decreases accuracy. The best results were obtained for the August 9 data which is an expected result. After the end of August maturation begins to occur and all crops start moving spectrally toward a uniform brown visible spectral characteristic and tend to loose their spectral separability. This is demonstrated by the decrease in classification accuracy with time exhibited in Tables 1c thru f.

The change in spectral characteristic can also be shown graphically by plotting mean relative spectral response for a large number of samples for the three dates. Figure 3 contains graphs of the mean spectral response for corn and soybeans for the three dates. The steadily decreasing infrared reflectance

Table 1 Classification Results for LARS ERTS Data Run 72032806
Spectral Data Northern Illinois Area

(a) Training Field Results - August 9, 1972

		% Correct Classification for Best N Channels N=1,4			
CLASS	No. POINTS	2	2&3	2,3,4	1,2,3,4
Corn	411	4.4	86.4	87.6	87.3
Soybeans	224	96.0	85.2	91.5	90.6
Other	217	79.3	88.5	91.7	94.0
Overall		47.5	86.6	89.7	89.9
Average Interclass Divergence		1313	1833	1867	1879

(b) Test Field Results - August 9, 1972

		% Correct for Best N Channels N=1,2,3,4			
CLASS	NUMBER POINTS	2	2&3	2,3,4	1,2,3,4
Corn	4848	12.9	81.4	76.2	76.3
Soybeans	793	78.6	83.9	85.2	84.9
Other	800	50.1	57.1	58.4	64.6
Overall		25.6	78.7	75.1	75.9

(c) Training Field Results - September 19, 1972

CLASS	NUMBER POINTS	% Correct for Best N Channels N=1,2,3,4			
		4	3&4	2,3,4	1,2,3,4
Corn	411	89.1	79.3	82.2	80.0
Soybeans	224	81.3	51.3	62.5	63.8
Other	217	23.0	49.8	52.5	53.9
Overall		70.2	64.4	69.5	69.1
Average Interclass Divergence		684	987	1119	1147

(d) Test Field Results - September 19, 1972

CLASS	NUMBER POINTS	% Correct for Best N Channels N=1,2,3,4			
		4	3&4	2,3,4	1,2,3,4
Corn	4848	69.2	59.5	58.9	56.6
Soybeans	793	72.5	46.3	58.1	52.5
Other	800	27.2	48.1	53.6	54.7
Overall		64.4	56.5	58.1	55.9

(e) Training Field Results - October 2, 1972

CLASS	NUMBER POINTS	% Correct for Best N Channels N=1,2,3,4			
		3	2,3	2,3,4	1,2,3,4
Corn	411	74.5	75.2	79.8	79.8
Soybeans	224	27.7	74.6	71.4	71.0
Other	217	85.7	87.6	87.6	87.6
Overall		65.0	78.2	79.6	79.5
Average Interclass Divergence		847	1175	1198	1220

(f) Test Field Results - October 2, 1972

CLASS	NUMBER POINTS	% Correct for Best N Channels N=1,2,3,4			
		3	2,3	2,3,4	1,2,3,4
Corn	4848	57.1	51.4	55.3	53.8
Soybeans	793	24.7	54.5	49.2	48.3
Other	800	65.2	65.7	68.8	71.6
Overall		54.1	53.5	56.2	55.3

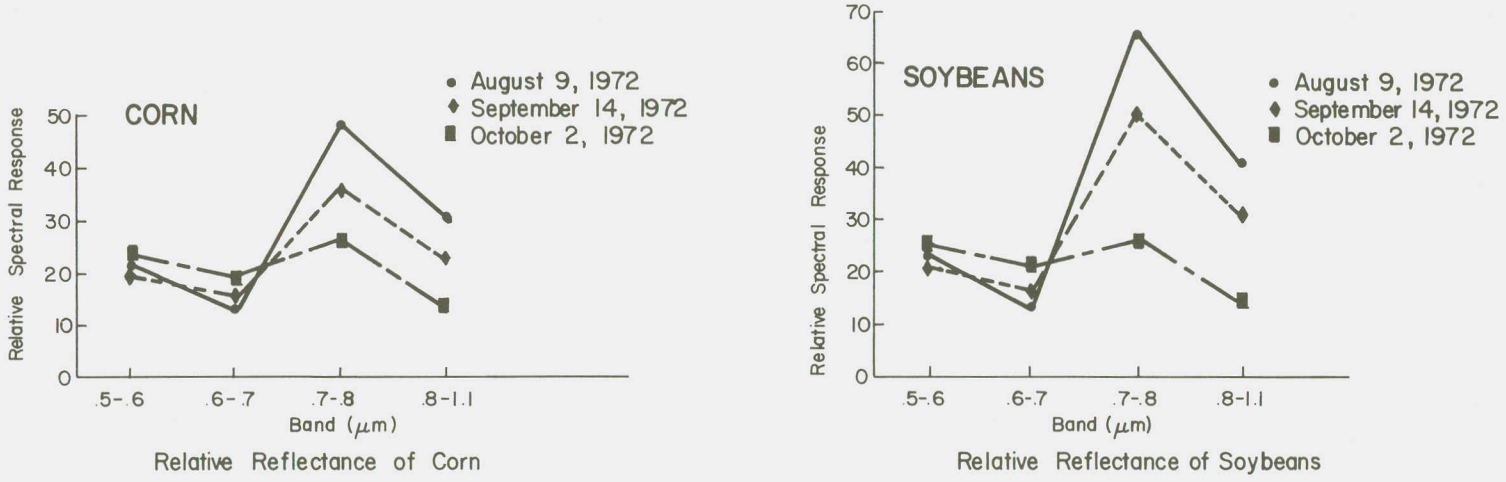

Figure 3. Mean ERTS spectral response for fields of corn and soybeans in Northern Illinois for three dates in 1972.

(.7-.8μ and .8-1.1μ bands) shows the loss of green leaf vigor due to drying and the increasing red wavelength band (.6-.7μ) values indicate the loss of chlorophyll absorption as the plants mature and dry. Temporal effects on separability can also be illustrated graphically by plotting mean spectral response for two bands with time as a parameter. Figure 4 contains such a response "trajectory" for the corn and soybeans training samples which shows dramatically how the distance between the classes decreases with time. Table 2 contains the mean responses for the two classes with the Euclidian distance

Table 2. Relative Spectral Responses of Corn and Soybeans, Northern Illinois test site: (LARS Run Number 72032806)

	August 9		September 14		October 2	
CHANNEL	CORN	SOYB	CORN	SOYB	CORN	SOYB
1	22.3	23.0	20.3	21.8	23.6	24.5
2	13.8	13.4	15.5	16.2	19.5	21.8
3	47.3	65.4	35.3	50.3	26.8	26.9
4	30.5	41.2	23.1	31.8	14.1	14.3
CHANNEL 2,3 DISTANCE	18.2		15.2		2.3	

computed for channel 2 and 3 between the two classes at the three times. These examples suggest that the third and possibly even the second times are not optimal for separation of the classes and indeed these data may reduce temporal classification accuracy.

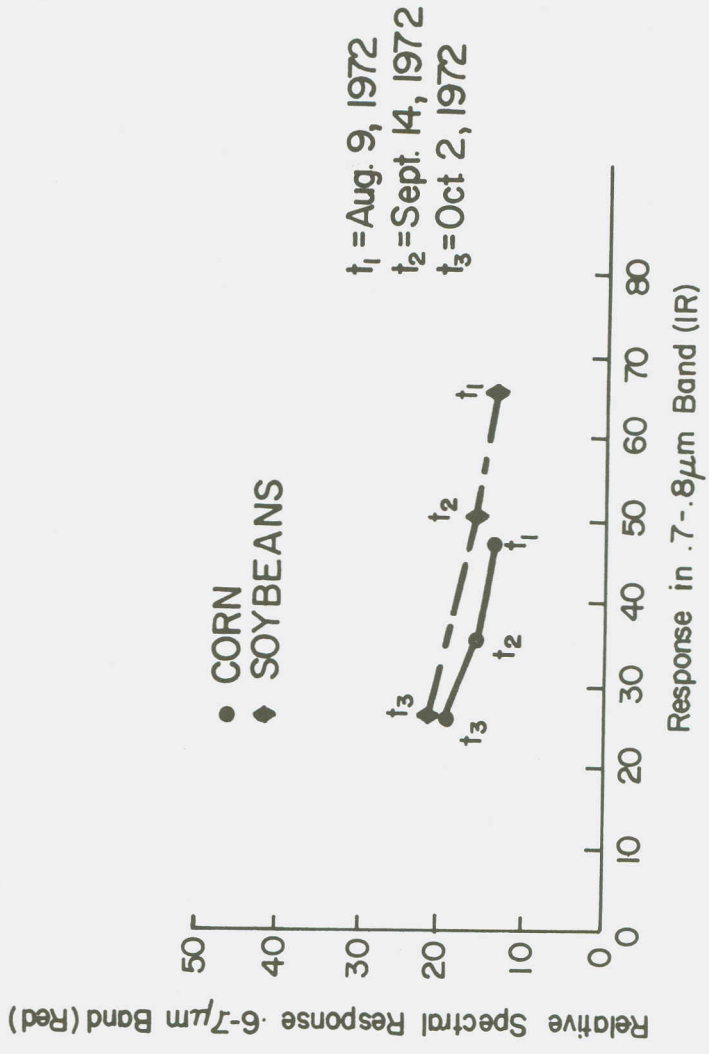

Figure 4. Mean ERTS spectral response values for two channels plotted as a function of time for fields of corn and soybeans in Northern Illinois, 1972.

Temporal classification experiments were conducted to explore this question further.

The twelve spectral/temporal channels were treated as one set of measurements and used to classify the same training and test samples used in the spectral experiments. Choosing the channels to use becomes the critical question since twelve channel classifications are excessively costly for large areas and there are a total of 4095 subsets of the twelve channels (i.e. all combinations of 1,2,...12 channels) to choose from. The LARSYS feature selection program was employed to select the best subset of four channels from the twelve available for spectral/temporal classification. First, the best four out of the twelve were determined and a classification was performed using the same training and test fields as before. The feature selection processor chose two channels from August 9 and two channels from September 19. The results for this experiment are included in Table 3. The training field accuracy increased by 3.5% while the test field results decreased 1.5% compared to the four channel August 9 results. The greatest influence on this decrease was the corn test accuracy decrease from 76.3% to 72.5%. The best six of the twelve available channels produced an increase in training accuracy of 5.3% but the test accuracy still was reduced, 2.5% in this case. All twelve available channels were also used and training accuracy increased only 4.5%, less than for the six channel case, and

Table 3. Training and Test Classification Results for Spectral/Temporal Analysis of Northern Illinois Test Site

TRAINING SAMPLE PERFORMANCE (% Correct Classification)

Class	Number Points	Best Aug 9 Result	Best Sept 19 Result	Best Oct 2 Result	Best 4 Channels of 3 Times	Best 6 from 3 Times	All 12 Channels from 3 Times	Best 4 Channels of Sept & Oct
Corn	411	87.3	82.2	79.8	92.9	94.6	92.7	92.0
Soybeans	224	90.6	62.5	71.4	96.0	96.0	96.0	86.7
Other	217	94.0	52.5	87.6	91.7	95.4	95.9	89.9
Overall	852	89.9	69.5	79.6	93.4	95.2	94.4	89.9

TEST SAMPLE PERFORMANCE (% Correct Classification)

Class	Number Points	Best Aug 9 Result	Best Sept 19 Result	Best Oct 2 Result	Best 4 Channels of 3 Times	Best 6 from 3 Times	All 12 Channels from 3 Times	Best of Sept & Oct
Corn	4848	76.3	58.9	55.3	72.5	73.0	68.4	64.6
Soybeans	793	84.9	58.1	49.2	82.2	83.5	81.0	76.1
Other	800	64.6	53.6	68.8	78.7	66.1	81.0	85.0
Overall	6441	75.9	58.1	56.2	74.4	73.4	71.5	67.8

test accuracy decreased 4.4%. These results suggest that straight forward inclusion of spectral measurements offering generally less spectral separability with a near optimum set of measurements will not improve the overall results of the classification. A correct temporal classification algorithm would use any new information made available by the temporal dimension and would not decrease classification accuracy if no new information existed in the new (temporal) data as was the case in these experiments. Thus, further study is required to define classification procedures which will make optimum use of the spectral and temporal measurements available.

The value of temporal data for improving classification results with non-optimal data was investigated. Assuming only September and October data were available, a classification analysis was run using the best four of the September and October channels. Table 3 also contains the results of this experiment. The test field accuracy using only September channels was 58.1% and the best October results were 56.2%. Using the best four channels from September and October which includes the spectral and temporal dimensions the test results were 67.8%. In this case, use of temporal data did have an appreciable beneficial effect on classification accuracy. Test results improved by 9.6% over the best of two purely spectral cases and were 11.5% better than the worst case. This result

suggests that there is some "crossover" point at which temporal data begins to improve classification results rather than harm them with reference to purely spectral classifications using data obtained only at one time.

The overall conclusion drawn from this experiment is that use of the temporal dimension will require more complex procedures than now used with multispectral data and further research into methods for utilizing this new data dimension is required.

IV. Use of Temporal Data for Change Detection

In this section a method is presented and tested for detecting change in multitemporal imagery. In the previous discussion the goal was to enhance multispectral crop classification accuracy by use of the temporal dimension. In this discussion the temporal dimension is applied to detection of change in the multispectral image. Two problems immediately arise from this statement: 1) What represents a change?; 2) What is a significant change and what is an insignificant change once a change has been defined and detected? What changes are of interest depends on who is making the inquiry. The urban planner is interested in new construction or at least large surface disturbance areas for observation of the rate and direction of urban expansion. An agronomist might be interested in changes in crop conditions for disease detection, assessment of maturation or observing the progress of harvesting. Hydrologists would be interested in changes in river width due to flooding or changes in riverbed location. A forester might be interested in changes in forest stands due to cutting, disease, fire, or landslides. The work presented here represents a beginning of technique development at LARS for change detection.

It is assumed that data to be analyzed for change is multispectral digital imagery obtained at a sequence of points in time over the same area. Image registration processing

is also assumed so that the starting point for this discussion is the registered multispectral imagery. The change detection problem can then be stated as follows:

> Given multispectral sample $X_{ij}(t_1)$ from line i and column j of a digital image at time t_1 and the sample $X_{ij}(t_2)$ at time t_2, determine if a change of interest (of informational value) occurred, i.e. are $X_{ij}(t_1)$ and $X_{ij}(t_2)$ different in some sense?

A multitude of techniques exist for testing whether or not $X(t_1)$ and $X(t_2)$ are the same. The simplest and most obvious method may be the most fruitful. That is elementary subtraction of the two values. Define the image delta function as:

$$\delta X(t_2) = X(t_2) - X(t_1)$$

The $\delta X(t_2)$ is thus the change in X_{ij} at time t_2 referenced to time t_1 with an increase resulting in a positive quantity. A significant change could be defined as any spectral difference value which exceeds a certain threshhold (T):

$$\text{Location i,j changed if } |\delta X_{ij}(t_2)| > T$$

Other methods make use of cell analysis where the cells contain a number of image points. Measures such as correlation, entropy and histogram analysis can be applied to the set of

points from corresponding cells obtained at different times. Kawamura [16] used techniques such as this to detect changes in urban areas. In addition to cell cross correlation and cell entropy a measure called high-intensity probability was developed by Kawamura to measure the extent to which a cell contains highly reflective objects. Cells used in his work were 64x64 points square covering 100 feet square areas on the ground. The cell correlation measure was the standard correlation coefficient:

$$r = \frac{\sum_{i=1}^{N}\sum_{j=1}^{N}(X_{i,j}(t_1)-m_1)(X_{ij}(t_2)-m_2)}{\sqrt{\sum_{i=1}^{N}\sum_{j=1}^{N}(X_{ij}(t_1)-m_1)^2 \sum_{i=1}^{N}\sum_{j=1}^{N}(X_{ij}(t_2)-m_2)^2}}$$

In this expression an N point square cell is assumed. The m_1 and m_2 represent the means of X at t_1 and t_2.

The cell entropy measure is an information theoretic function representing the degree of spread in the intensity distribution and hence the amount of randomness in the cell. For a cell of N^2 points having an intensity distribution H_k over k=1,...M intensity levels the average entropy for the cell is:

$$P = -\sum_{k=1}^{M} H_k \log_{10} H_k$$

Where H_k is the histogram derived intensity distribution for

the cell with $\sum_{i=1}^{M} H_k=1$. The entropy P at time t_1 at time t_2 is computed and the two values compared to determine if changes have occurred. An increase in entropy indicates that more randomness was introduced into the scene.

The high-intensity probability is the probability that objects have an intensity higher than level k and is computed as:

$$h= \sum_{i=k}^{M} H_i$$

These three measures were used by Kawamura in a three dimensional pattern recognition experiment to detect changes, e.g. changes in the presence of buildings, streets, parking lots and trees in an urban scene. Although these methods show promise for change detection in aerial photography the resolution of ERTS images is such that one cell covers a large area (79 meter square) and testing blocks of cells for change would tend to mix such a large number of surface objects that little useful information would be obtained - at least in urban areas. Thus the work reported here was directed toward determining change in individual image elements. The Gaussian maximum likelihood classification algorithm used in part II was used to classify the difference image into two or more classes of change. Computer printer maps were produced containing the change decision for each image point. The results were then manually checked against

the actual environment producing the spectral data.

Representation of Multispectral Changes

The difference or delta transformation combines two n channel multispectral images obtained at different times and produces a multispectral delta image having n channels. Most image processing systems assume all image samples are non-negative and this is true for the LARSYS system used in this study. To handle negative differences a bias is added to each difference so that the resulting delta image is non-negative. Thus the complete transformation is simply:

$$\delta X_{ij}^{k} = X_{ij}^{k}(t_2) - X_{ij}^{k}(t_1) + b_k$$

Where: X_{ij} Defined Previously $i,j=1,\ldots N$ Assuming an NxN image

i Row

j Column

k Channel

b_k Bias for Channel k

The method proposed here for detection of change follows a procedure similar to that for classification of multispectral data. Indeed, change detection could be accomplished by classifying the multispectral data at time t_1 and t_2 and then comparing the results for differences. The method set forth here emphasizes multispectral change classification rather than changes in multispectral classification. Implementation of an automatic scheme in either case would require image

registration. A comparison of steps for the two approaches is:

Change Detection in Delta Images	Observation of Change in Classifications
1. Temporal Image Registration	1. Cluster Analysis at time t_1
2. Delta Transformation	2. Train Classifier for time t_1
3. Cluster Analysis	3. Classify time t_1
4. Train Classifier	4. Cluster Analysis at time t_2
5. Classify Delta Imagery	5. Train Classifier at time t_2
	6. Classify time t_2
	7. Register Classifications
	8. Process Classifications to Determine Changes

In addition to requiring less steps the Delta Image method may require less training activity since all features that do not change do not have to be isolated and described. The method proposed here uses non-supervised classification (clustering) to identify samples characterizing various change conditions. These samples are used to train a supervised classifier to classify each delta image point over an arbitrarily large area. The results can then be displayed in map form and tabular form the same as for the crop classification case.

The test area chosen for study of the evaluation of the change detection technique is central Tippecanoe County, Indiana. A topographic map photograph of the center county area is presented in Figure 5. The map covers an area of approximately

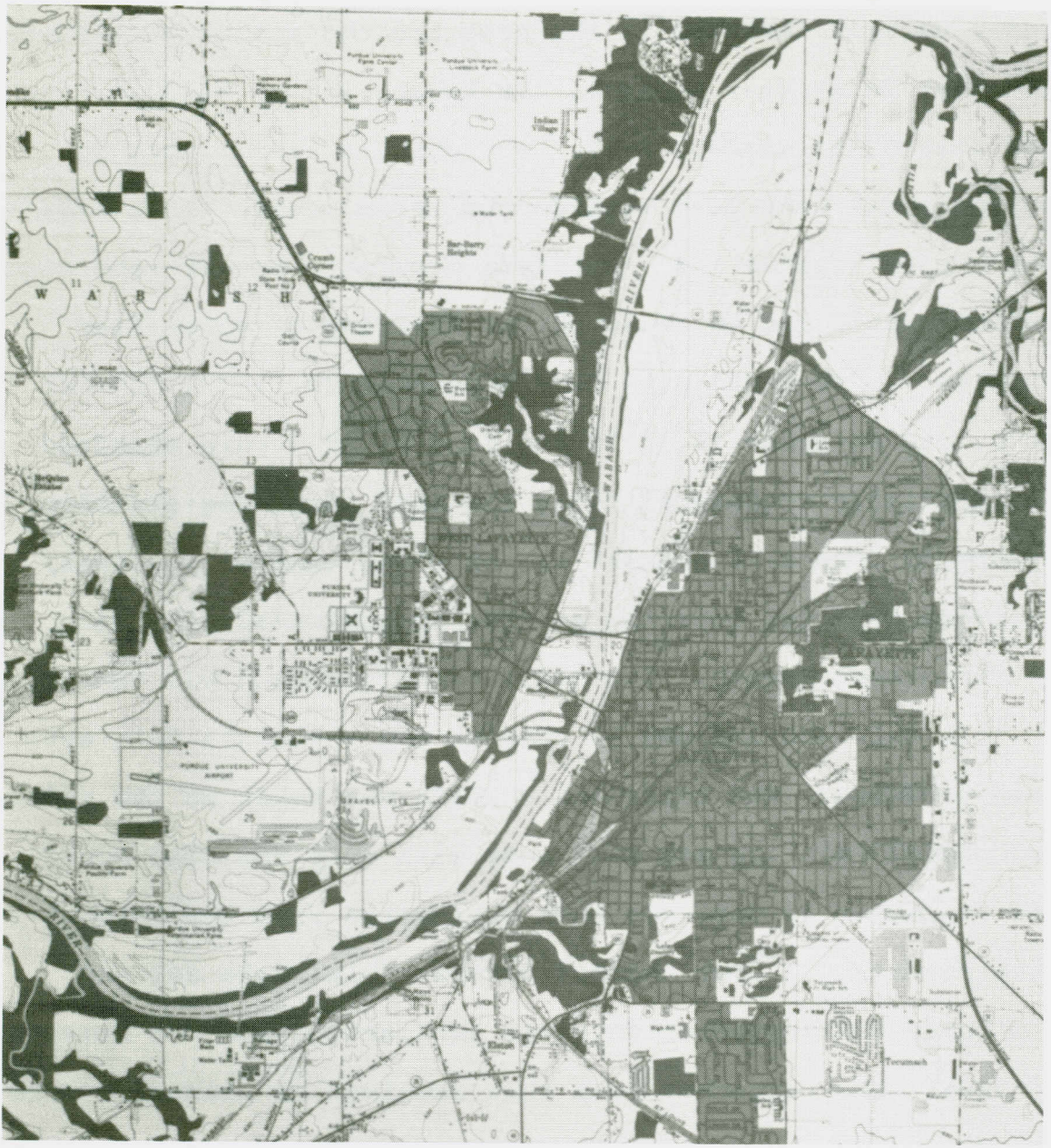

Figure 5. USGS Topographic Map of Change Detection Test Site. Lafayette, Indiana East and West 7 1/2 minute quadrangles.

12x8 = 96 square miles (19.3 x 13 = 250 square kilometers). The prominent features in the area are the cities of Lafayette and West Lafayette, Indiana, the Wabash River, Wildcat Creek, and Interstate Highway I-65. The area is almost totally agricultural crop land outside the urban areas. This area was chosen because its immediate proximity to our laboratory enabled rapid and detailed manual checking of classifier results. ERTS-1 MSS data from September 30, 1972, October 19, 1972, and November 24, 1972 and June 9, 1973 were obtained and spatially registered using the LARS image registration system to form a 12 channel and an eight channel spectral/temporal data set covering an area approximately the size of Tippecanoe County. The delta transformation was then applied to this data set and new 12 channel and 8 channel data sets were produced. The September 30 data was taken as the reference and copied onto the new data sets with only the bias added. The September 30 data was then subtracted from the October 19 data producing a four channel October delta data set and similarly the September data was subtracted from the November 24 data. The September data thus remained as channel 1 thru 4; the October delta data became channels 5 - 8 and the November delta data became channels 9 - 12 of one data set. Another data set contained the September data as channels 1 - 4 and the June delta data in channels 5 - 8. A digital image display reproduction of the .6-.7 micrometer band is presented in

Figure 6 for the four times. Figure 7 contains image reproductions of the October, November, and June delta channels for .6-.7 micrometer band.

The brightness levels in the delta images of Figure 7 indicate relative increase or decrease in reflectance in the red wavelength band for each image point. The dynamic range of the ERTS data is 0 to 127 and the data is stored in eight bit words giving a possible data range of 0 to 255. Thus the bias was set at 128 for all channels (b_i=128 i=1,2,...12). The maximum change cannot overflow the number system with this choice. Thus, if delta channel values of 128 are observed no change took place in the received energy for that element. If a value greater than 128 is observed the reflectance increased and if less than 128 a decrease took place. This relationship is complicated by the fact that solar illumination intensity is decreasing with time in the Fall and increasing after the Winter solstice so that even if no change in reflectance of a picture point took place the reflected energy from the point would change. The gray scale images in Figure 7 offer a visual representation of relative change only and no absolute change information is available. The darker gray areas in the delta images are the Wabash River, Interstate 65 and relatively or totally treeless urban areas. These areas have relatively constant reflectances. These features and

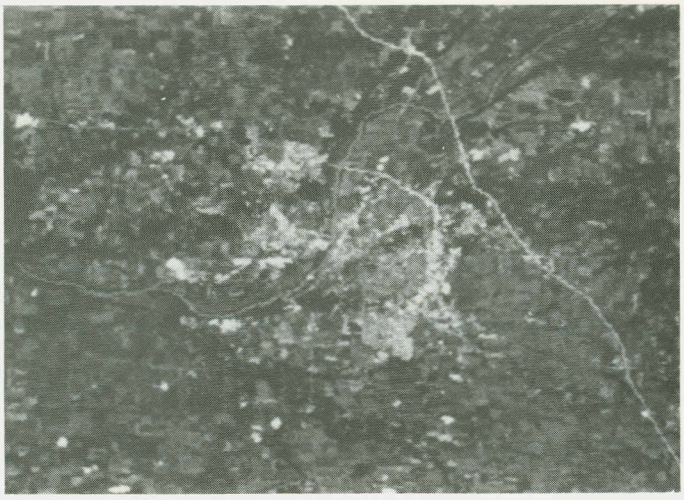

Figure 6a. ERTS-1 Data in .6 to .7 micrometer Band of Lafayette, Indiana on September 30, 1972.

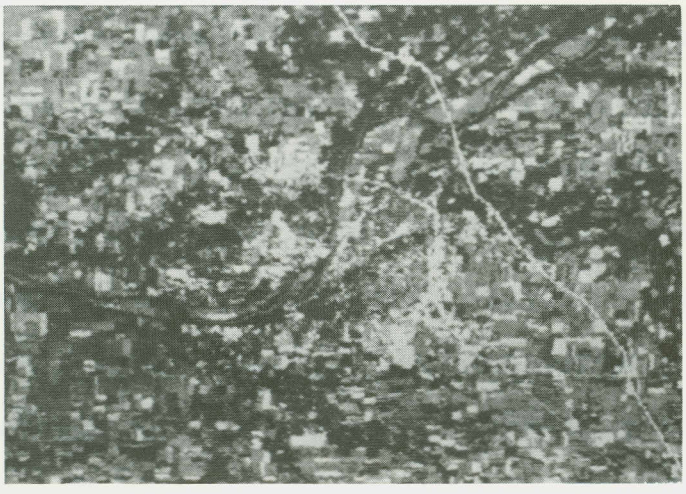

Figure 6b. Same details as 6a except data is October 19, 1972.

Figure 7a. September 30, 1972 Image Subtracted from October 19, 1972 Image. Channel 2 (.6-.7 micrometers).

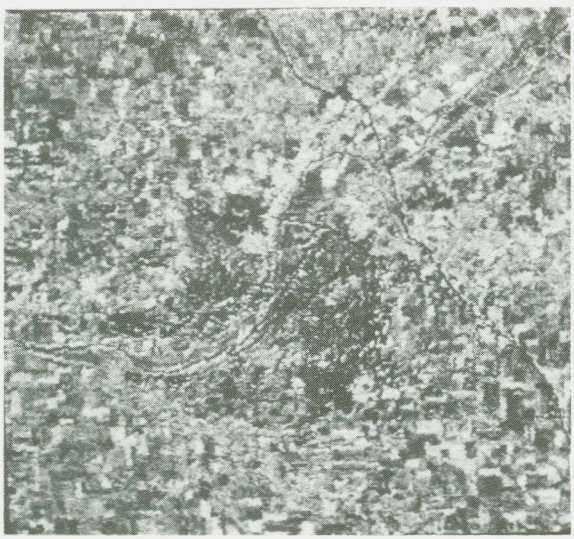

Figure 7b. September 30, 1972 Image Subtracted from November 24, 1972 Image. Channel 2 (.6-.7 micrometers).

Figure 7c. June 9, 1973 Delta Image. September 30, 1973 image was subtracted from June 9 image. Channel 2 (.6-.7 micrometers) shown.

associated gray tones are assumed to represent the no change condition. The black and very dark gray regions signify a decrease in reflectance and the bright regions signify increases in object reflectance.

Many of the agricultural areas appear light gray or white in the delta images indicating an increase in reflectance due to maturation and browning of the corn, soybean and other plants in the Fall and bare soil exposure in June. The October delta image is generally dark with many isolated bright fields. Ground checking indicated that the majority of the very bright fields were corn and it is hypothesized that the plants were turning brown and losing their chlorophyll absorption property thereby increasing the reflectance in the red wavelength region. Numerous bright spots of one or two points each are observed especially along the Southern edge of the city of Lafayette (note the horizontal line of white spots in the center of the October delta image, below the very dark Lafayette City area). This is a predominately older residential area along the North side of Teal Road which is a heavily forested area and includes the Tippecanoe County Fairgrounds. The Fairgrounds are covered with a stand of large oak trees which are starting to turn color and possibly decreasing their leaf density so that more bright concrete pavement or house-tops show through. The November 24 delta image indicating change over 55 days is very bright throughout

the agricultural area indicating widespread maturation of the soybeans and corn and increasing exposure of highly reflective soil. Many parts of the urban and residential areas show spotty or general brightness indicating tree coloration, defoliation and exposure of underlying concrete and roof areas. The forested areas in Happy Hollow and along the hill and high ground along the West Wabash Riverbank North of the city are extremely bright which could be due to dry leaves remaining on the dense forest scene. The June 9 delta image shows most fields as extreme white indicating dry bare soil is present where mature crops or crop residues existed on November 30. The dark areas along the streams are forest stands which have decreased in reflectance compared to November 30. From this discussion it can be seen that vegetation has a dominant impact on spectral reflectance change and urban changes may be masked and confused by vegetation changes.

Two change detection goals are set forth for this study. The first is to detect and map maturation in predominant crop types (corn and soybeans) in the test area. The second goal is to detect urban change due to large new construction projects. The large (79 meter) resolution element size for ERTS would apparently prevent discrimination of single house or small commercial construction sites but large housing or commercial-industrial changes involving many resolution

elements are candidates for change detection from ERTS data. The detection of these changes is pursued by use of both non-supervised and supervised digital pattern classification techniques. Due to the short time interval between the Fall 1972 coverages and the slow rate of urban change it was decided that crop maturation would be studied in the October or November delta data and urban change would be studied in the September 30, 1972 to June 9, 1973 delta image. The eight month period between the September - June data enabled many construction projects to be ground-truthed and located in the imagery. Two test sites were chosen in the area shown in Figure 6 for change detection study. An agricultural site was chosen in the Northeast quadrant of the area covering an area of about 7 km x 7 km = 49 square kilometers. An urban test site was chosen centered on downtown Lafayette and covering an area of 7 km x 8 km = 56 square kilometers.

Non-Supervised Analysis of Spectral/Temporal Data

The clustering algorithm was applied to the spectral data for the two test sites in order to generate a base map of cover type for analysis of change detection results. (Both test areas were first clustered using spectral rather than delta data.) The selection of the number of clusters and the channels to be used was the first problem encountered. To find the correct number of clusters in the data, the number of clusters specified was varied from twelve down to six.

This choice was based on the assumption that there were at least six classes in the agricultural site: Corn, soybeans, grass, trees, water, residential/commercial, and at least six classes in the urban site: Downtown, industrial, 30 - 70 year old residential, 1 - 30 year old residential, trees, and water. Starting the cluster analysis at twice the expected number of clusters and "collapsing" the data set into fewer and fewer clusters enables the metrically "optimum"* number to be chosen from the average quotient, $\overline{Q}$, and the minimum value of all pairwise quotients (Qmin) parameters. The channels used were bands 2,3,4 from September 30 spectral bands in one case and two September 30 plus two October 19 bands in another. Temporal data was tested for improved clustering by using September and October channels together. (Channels 2 and 4 from September and October were chosen.)

The $\overline{Q}$ and Qmin values for each clustering operation are listed in Table 4 for the urban and agricultural test sites. The $\overline{Q}$ for the urban site holds around 1.7 down to 10 clusters and then drops sharply to 1.3 at 9 clusters for the September data. The Qmin also drops .75 to .47 at 10 giving a strong

---

* Optimum here is in reference to the technique of examining the $\overline{Q}$ and Qmin results and is only a local optimum if all methods of cluster analysis are considered.

Table 4 Cluster Separability Data for the Agricultural and Urban Test Sites.

	URBAN SITE				AGRICULTURAL SITE			
	September Bands 2,3,4		Sept. 2,4 Oct. 2,4		September Bands 2,3,4		Sept. 2,4 Oct. 2,4	
Number Clusters	$\bar{Q}$	Qmin	$\bar{Q}$	Qmin	$\bar{Q}$	Qmin	$\bar{Q}$	Qmin
12	1.8	.72	1.4	.60	1.5	.63	1.1	.61
11	1.7	.73	1.4	.59	1.5	.61	1.1	.53
10	1.7	.75	1.4	.63	1.5	.65	1.1	.50
9	1.3	.47	1.1	.60	1.4	.62	1.0	.51
8	1.1	.46	.95	.53	1.4	.72	1.0	.48
7	1.1	.47	.96	.48	1.3	.71	1.0	.60
6	1.1	.53	.93	.57	1.3	.76	.90	.59

indication that 10 is the desired number of clusters for the urban site. The results using the September + October data tend to reinforce this choice. The $\bar{Q}$ for the agricultural plot using September data remains high for all clustering operations but the Qmin rises with decreasing number of clusters and is above .75 at 6 clusters. The results using September plus October data are inconclusive since the $\bar{Q}$ and Qmin change very little with number of clusters. The "optimum" of 6 indicated by the Qmin and $\bar{Q}$ results for September data was chosen for the agricultural test site analysis.

The September data cluster map for the urban and agricultural sites were annotated with roads and some natural features to serve as reference for the change detection analysis. The annotated cluster map is presented in Figure 8 for the agricultural site and Figure 9 contains the September data cluster map for the urban site. These maps were used to help select training fields for supervised classification of the sites. The cluster map for the urban site includes locations of major construction projects observed during the September 30, 1972 - June 9, 1973 period. These observed changes are identified in Figure 9 by numbers and are described in Table 5.

Table 5 Urban Construction Projects Started or in Progress during September 30, 1972 - June 6, 1973 Period.

I.D. NUMBER	DESCRIPTION	APPROXIMATE AREA
1	Hilton motel and shopping center construction along Route 52 North. Started about November 1972. Area previously agricultural field. Cover unknown on September 30, 1972.	660 x 660 FT
2	Apartment construction project "The Seasons" at corner of Yeager Road and Cumberland Avenue, West Lafayette. Started clearing ground Spring 1973. Apartment buildings erected July - August 1973. Area previously idle, covered with weeds and brush.	660 x 330 FT
3	Golf course construction along Wabash River North of Lafayette. Grading and earth hauling in progress through 1972 and 1973. Area previously corn and soybean fields and included small airstrip.	1980 x 5000 FT
4	AyrWay Shopping Center construction along Route 52 by-pass South, Lafayette. Started Fall 1972. Area previously golf range (grass).	600 x 600 FT
5	Condominium and housing construction in Pipers Glen Addition on Brady Lane on South side of test site. Most houses in place September 1972 but row of condominiums started after September 30, 1972.	2000 x 1300 FT
6	Apartment construction near Northwest corner of Brady Lane and Road 250 East.	600 x 600 FT
7	Construction of addition to Wabash Valley Sanitarium, Road 43 North. Fall 1972.	600 x 400 FT
8	Housing addition under construction during period.	500 x 1000 FT

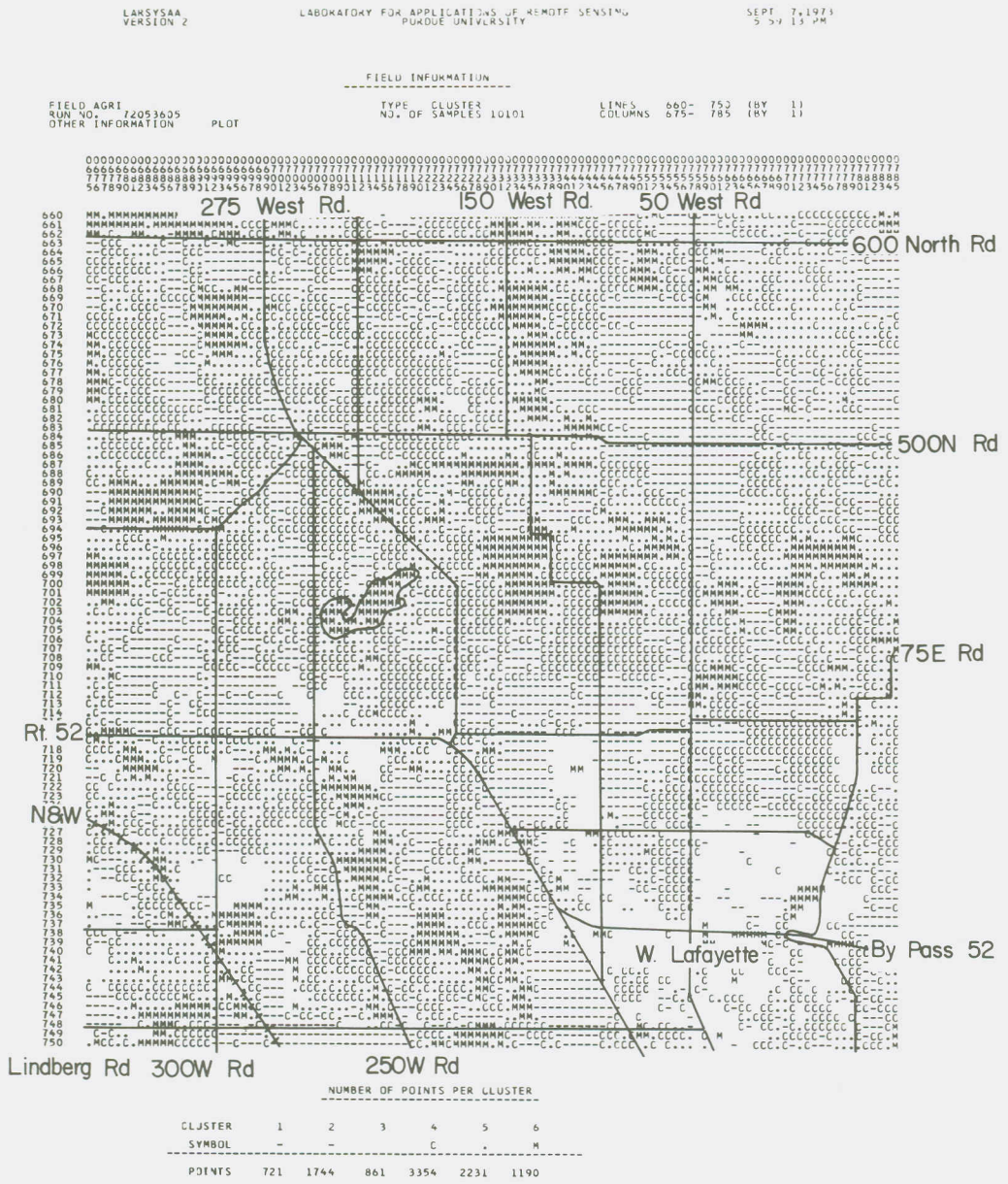

Figure 8. Non-supervised classification (clustering) printout of agricultural change detection test site. The .6-.7 μm .7-.8 μm and .8-1.1 μm bands from September 30, 1972 spectral data were used. (μm = micrometer) Cluster-symbol relationship is given below the printout.

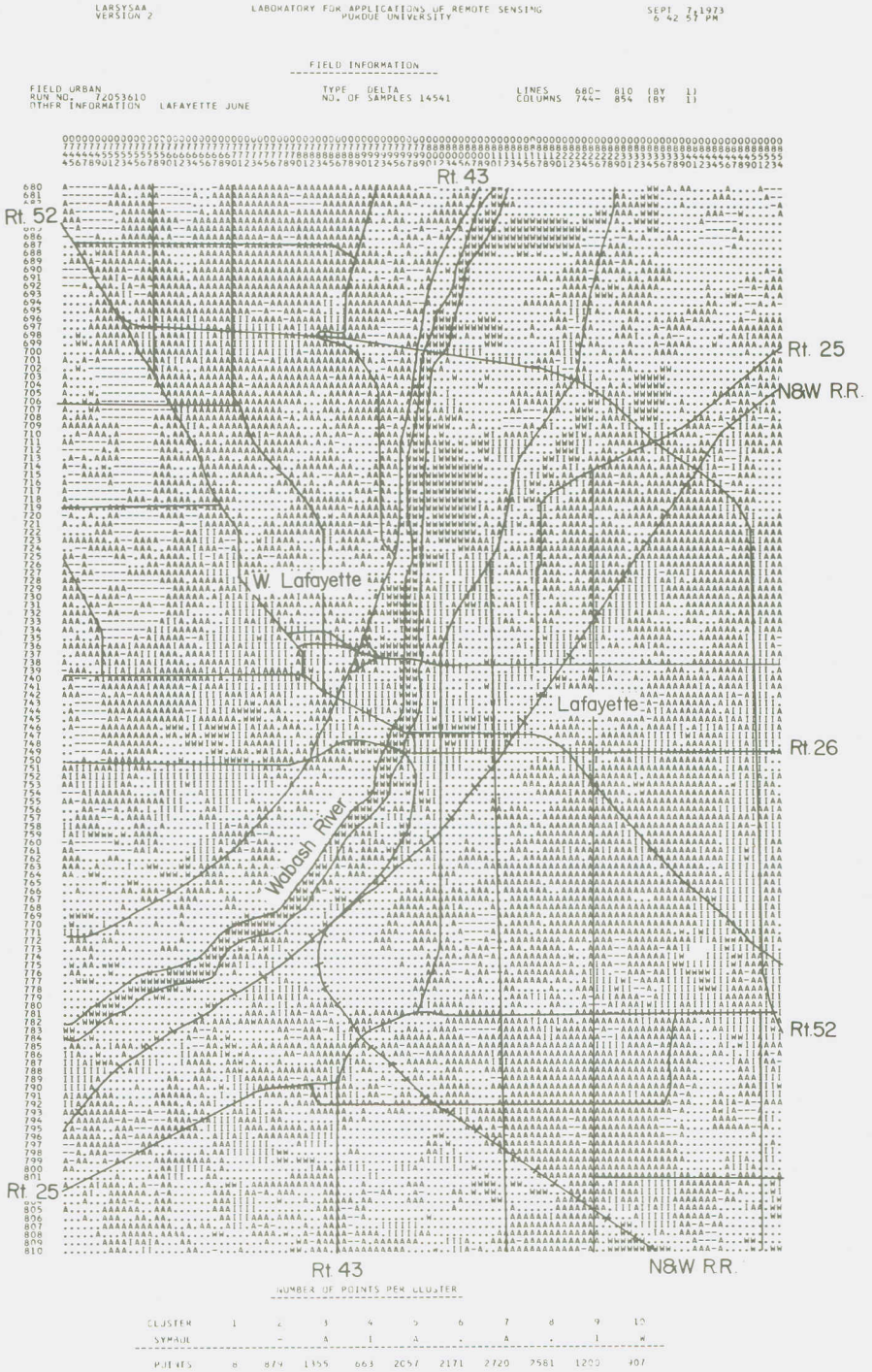

Figure 9. Non-supervised classification (clustering) printout of urban change detection test site. The .6-.7 μm, .7-.8 μm and .8-1.1 μm spectral bands were used. (μm = micrometer) Cluster-symbol relationship is given below the printout.

Supervised Classification of Spectral/Temporal Data

The cluster maps were used to aid in selecting training fields for the Gaussian maximum likelihood (GML) classifier. Training fields for six classes in the agricultural site and ten in the urban site were chosen, the classifier was trained, and the test sites were classified. The classification maps for the agricultural and urban sites were used to aid in checking the change detection results.

Next, the GML classifier outputs were inspected for quality of classification. Figure 10 contains the classification map for the agricultural area. It was noted that for the agricultural site water (Hadley's Lake) was separated from soybeans and classified accurately whereas the cluster process could not separate these features at all. Many fields known to contain corn and soybeans were confused with each other, however. The quality of the crop classification was not as high as desired for the test because of extremely wet conditions on the November 30, 1973 period. Heavy rains fell on November 28 and the soil was very wet. A large amount of standing water existed in the area. This condition undoubtedly adversely effected the evaluation of the change detection results. No earlier data was available which could have produced a better reference crop classification.

When the cluster results for the urban area were inspected for relationships to known surface categories, corn

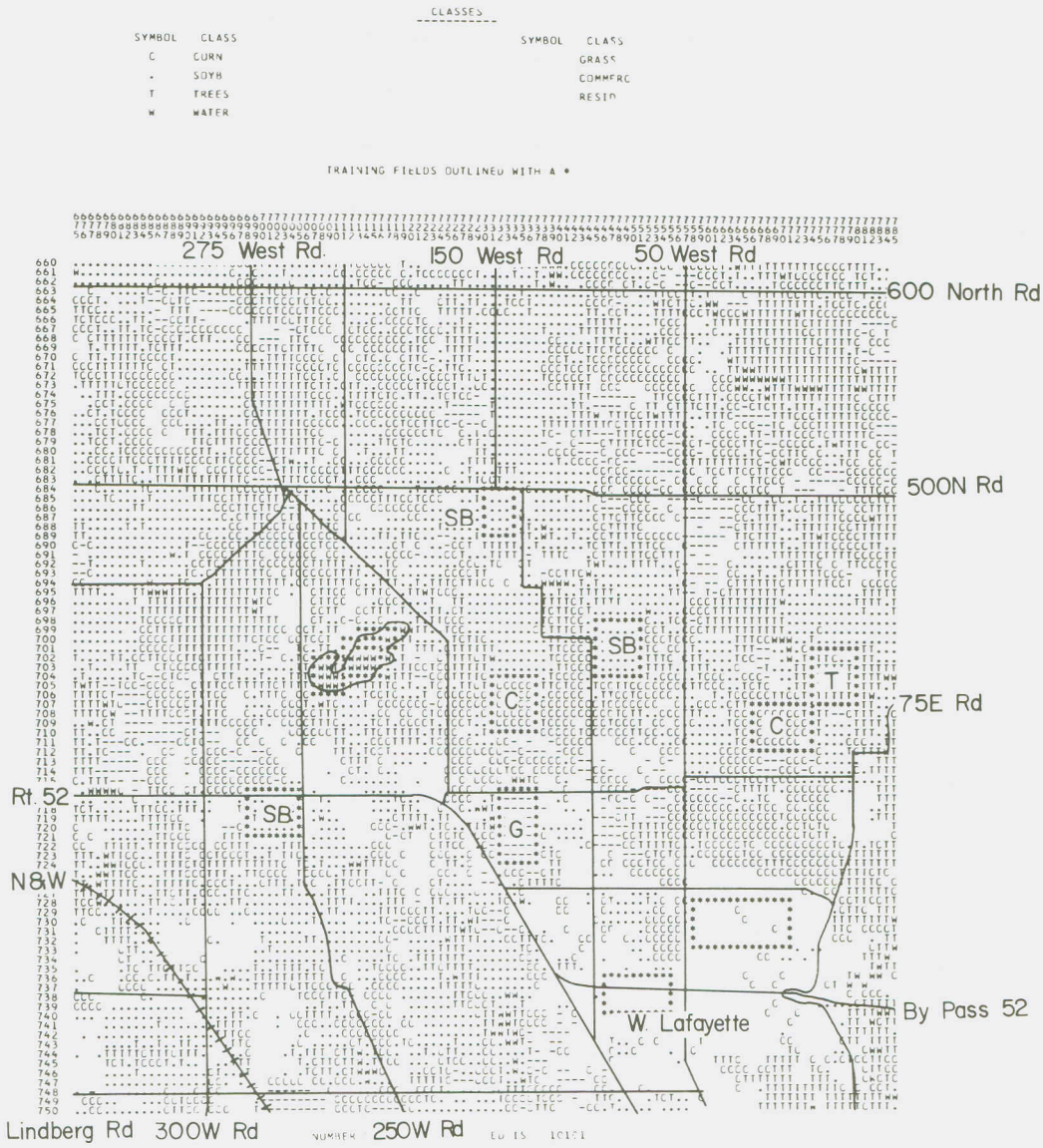

Figure 10. Supervised classification of agricultural test sites using spectral data. Bands .5-.6 μm, .6-.7 μm, .7-.8 μm, .8-1.1 μm used. (μm = micrometer). Relationship between symbol and class is given above printout. Ground truth data added to printout with symbols as follows:
C=Corn, SB=Soybean, G=Grass, T=Trees.

fields bordering the urban areas were observed to cause mixing with residential areas so an additional cluster (corn) was defined. Samples from the eleven clusters were selected and used to train the supervised classifier and the resulting map is presented in Figure 11. Visual inspection of the results within the general city boundaries indicated good classification accuracy. Outside the urban area corn fields are being heavily classified as commercial and downtown. The corn field North of West Lafayette used for the corn training caused good accuracy of corn classification in the immediate area but corn was not accurately recognized elsewhere. The performance of the classifier on the urban classes of residential, commercial/ downtown, forest, grass, and water was acceptable for purposes of this study.

Non-Supervised Analysis of Delta Images

The clustering algorithm was next applied to the delta images for the two test sites. Again the number of clusters to specify and channels to be used had to be decided on. Two approaches were taken with regard to number of clusters. First the number of clusters was arbitrarily set at three to represent conditions of no change, moderate change, and large change to get a quantative "feel" for the delta form of data. Next the "collapsing cluster" approach was used to determine how many separable clusters existed in the delta data. In the three

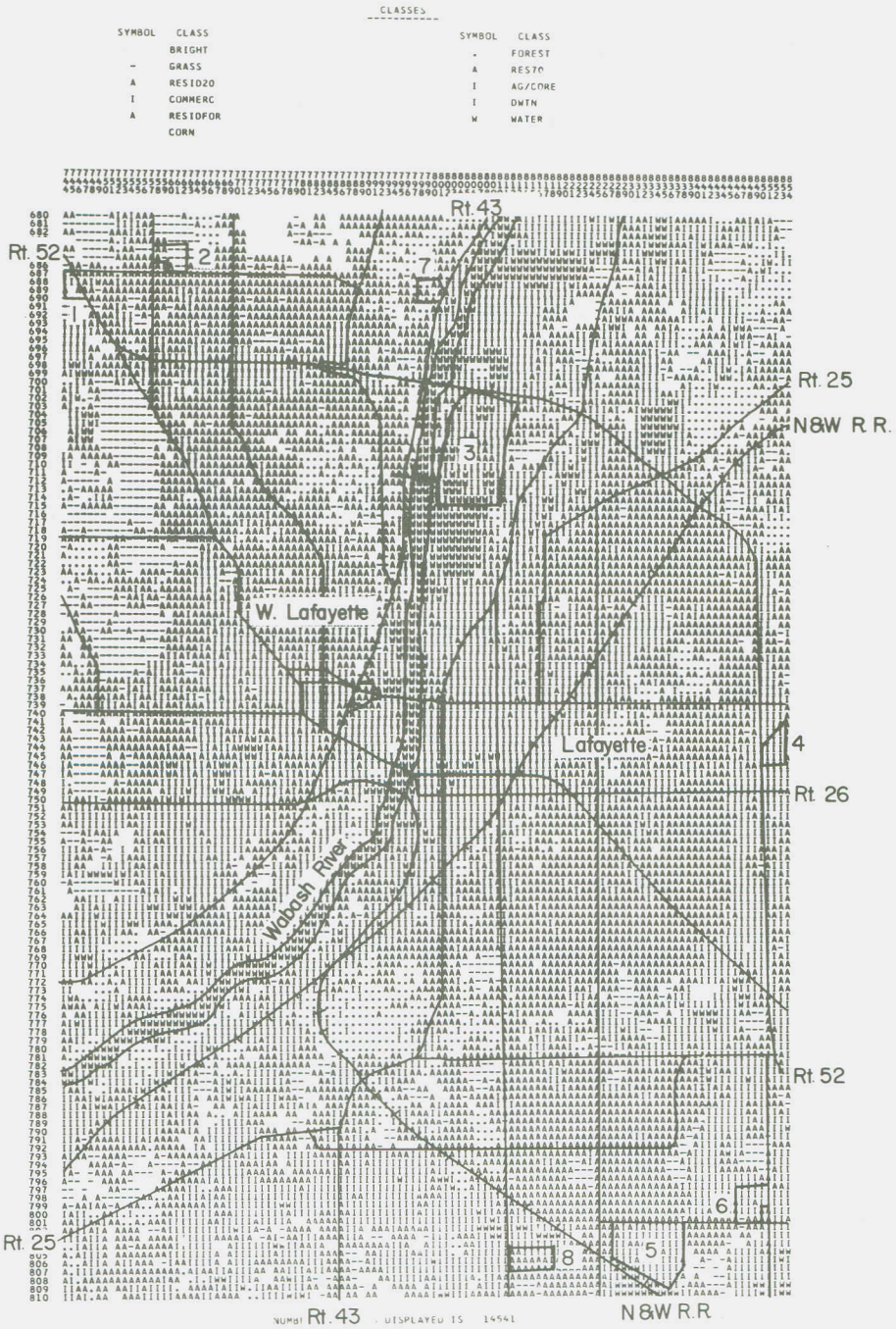

Figure 11. Supervised classification of urban site using spectral data. Same four bands used as in Figure 10. Class symbols explained above printout. Construction sites annotated by numbers 1 through 8.

cluster analysis only the red band (.6 - .7 micrometers) was used and in the second method three channels were used (.6 - .7 micrometers, .7 - .8 micrometers, .8 - 1.1 micrometers).

The three cluster map for the October delta data for the agricultural site is presented in Figure 12 with roads drawn in. The cluster having the largest mean is indicated by plus signs, the intermediate cluster by a blank and the lowest mean cluster by a minus sign. Figure 13 contains the three cluster map for the urban site for the June 1973 delta data. Table 6 contains the cluster mean and variances for only the urban site for all three delta image dates. Note that the values of the means tend to drop in October and November and rise in June. This is due to the effect of solar elevation mentioned previously in addition to changes in scene reflectance. It is assumed that water, highway and downtown areas represent no change conditions. These areas fell in cluster 3 in the October and November delta image clustering results and the downtown area tended to fall in cluster 2 in

Table 6 Cluster Statistics for October, November and June for Single Channel (.5 - .6 micrometers) Clustering of delta Images for the Urban Test Site.

Cluster	October 19, 1972		November 24, 1972		June 9, 1973	
	Mean	Variance	Mean	Variance	Mean	Variance
1	132.0	6.4	129.6	3.5	158.6	45.5
2	127.4	1.1	124.7	2.9	142.4	9.0
3	122.9	11.1	117.4	30.7	135.3	13.0

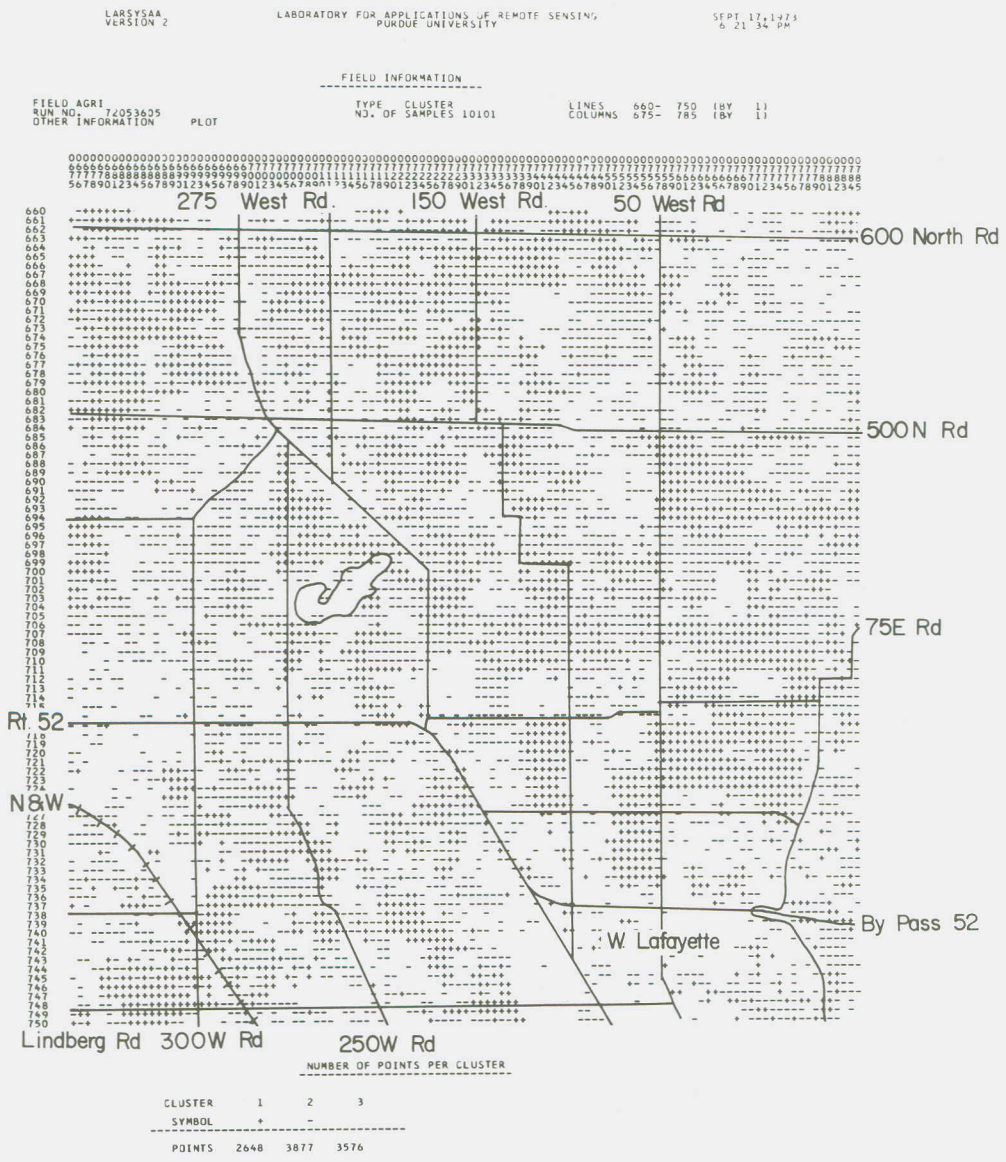

Figure 12. Non-supervised classification (clustering) of agricultural site using delta data. Only .6-.7 μm delta band from October 19 used. Cluster 1 (+ signs) is related to points having greatly increased reflectance and cluster 2 (- signs) relates to points having moderately increased reflectance compared to September 30. Cluster 3 (blanks) represents no change.

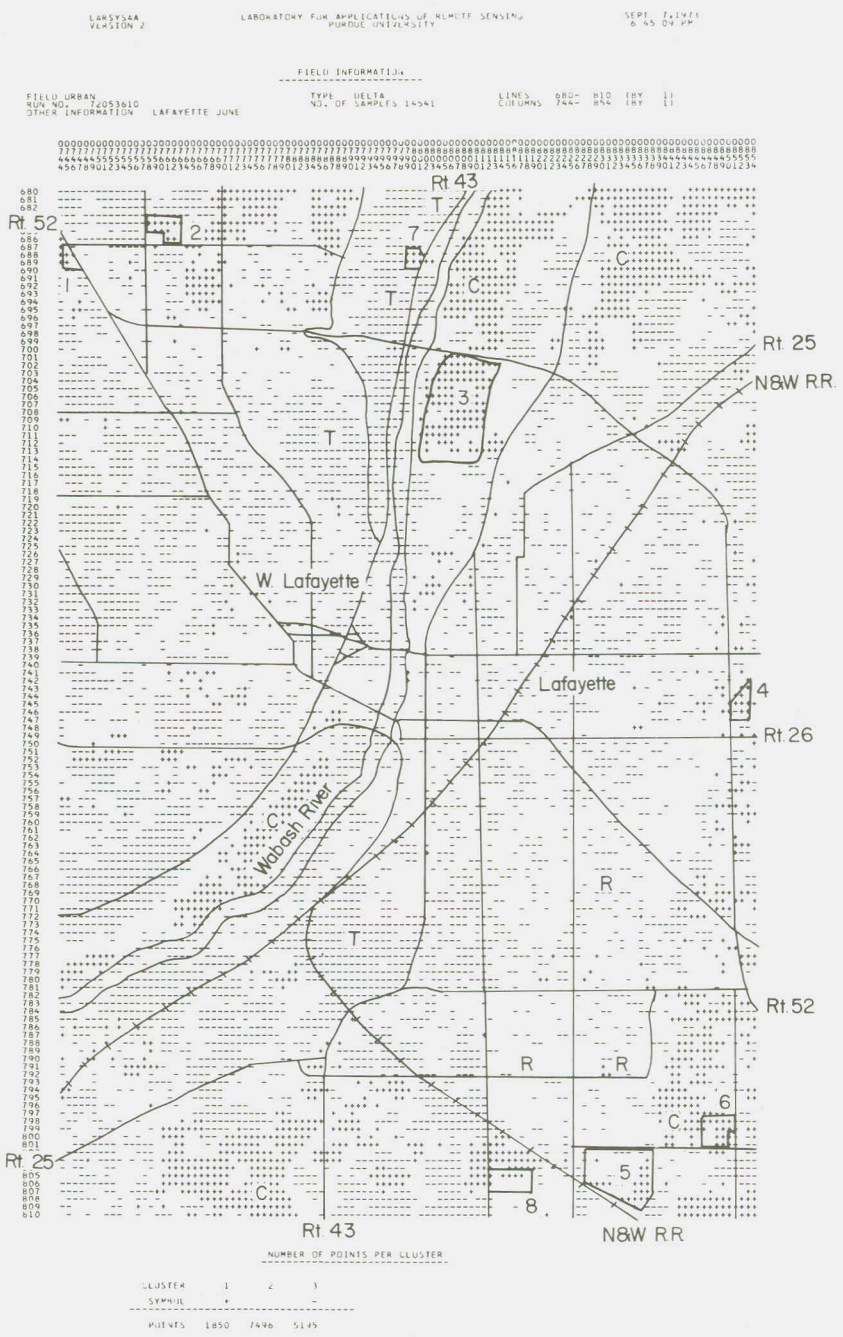

Figure 13. Non-supervised (clustering) classification of urban test site using delta data. Only the .6-.7 μm delta band from June 9, 1973 used. Cluster 1 (+signs) represents points increasing in reflectance, Cluster 2 (blank) represents no change and Cluster 3 (-signs) represents decreased reflectance compared to Septmber 30, 1972.

the June delta clustering results. It was hypothesized that the low mean cluster (No. 3) represented the no change conditions for October and November and for June 9 cluster 2 is assumed to represent no change.

A heuristic evaluation of the assertion that the low or intermediate cluster represents the no change condition can be obtained by examining the solar elevation angle θ and atmospheric path lengths for the four data collection dates. Assuming a spherical earth of radius R_e with an atmosphere of constant density of height H_A the solar path length L as a function of solar elevation is:

$$L = -R_e \sin\theta + \sqrt{R_e^2 \sin^2\theta + H_A(2R_e + H_A)}$$

A tabulation of the angles, length ratios and estimated effect on cluster means is presented in Table 7. The approximated atmospheric path length is 14% greater on October 19, 55% longer on November 24, and 25% less on June 9 compared to November 30. The increase in path length would reduce scene

Table 7 Estimated and Observed Change in Cluster Mean for Four Dates.

DATE	SOLAR ELEVATION	PATH LENGTH RATIO	PREDICTED CHANGE DUE TO PATH LENGTH CHANGE	CLUSTER 3 MEAN CHANGE (OCT, NOV) (CLUSTER 2 FOR JUNE)
Sep 30	41°	1	0	0
Oct 19	35°	1.14	-3.1	-5.1
Nov 24	25°	1.55	-9.2	-10.6
Jun 09	61°	.75	+8.6	+14.4

illumination to 88% of the September 30 level by October 16 and 64.5% by November 24 assuming linear attenuation by the atmosphere. The June 9 illumination would be 33% greater. The all class mean for the September 30 data before delta transformation was 26.0 and these factors suggest a 3.1 level reduction in this mean by October 19, a 9.2 reduction by November 24, and an 8.6 level increase for June 9, 1973. The change observed in cluster 3 (Table 6) was -5.1 for October, -10.6 for November and +14.4 for the June cluster 2 which agrees sufficiently with the path length estimation to reinforce the choice of cluster 3 for October, November and cluster 2 for June as the no change cluster. The June es estimate appears to be conservative suggesting that the atmospheric effect is non-linear and that a specular effect is being observed for the downtown structures. It was concluded that a change of nominally -5.1 for October 19, -10.6 for November 24, and +14.4 for June 6 could be attributed to solar elevation changes.

Multispectral as opposed to single channel clustering was next carried out on the delta data for October 19 and June 9 cases. In the agricultural scene, five types of changes were hoped to be differentiated: Change in corn fields, change in soybean fields, change in trees, miscellaneous changes (grass, weeds, etc.) and no change. To determine the

number of clusters in the data, the site was clustered using ten down to three clusters. The urban site was examined for six types of change: Construction projects changing grass-weeds to bare soil; Construction causing grass-weeds to change to built-up status (roofs, concrete, macadam, grass); Crop cover changed to plowed bare soil; Tree (forest) change; miscellaneous change; and no change. The urban site was clustered using from 12 down to three clusters. The $\overline{Q}$ and Qmin for these cluster calculations are presented in Table 8. The average Q drops significantly, going from nine to eight

Table 8 Cluster Separability Data for Multispectral Delta Images.

	Agricultural Site		Urban Site	
Number of Clusters	$\overline{Q}$	Qmin	$\overline{Q}$	Qmin
12	----	---	1.82	.65
11	----	---	1.19	.63
10	1.25	.57	1.14	.57
9	1.23	.63	1.14	.62
8	1.12	.56	1.10	.58
7	1.06	.56	1.04	.63
6	1.12	.58	1.01	.63
5	1.08	.65	.90	.59
4	1.04	.69	.86	.64
3	.81	.69	.75	.62

clusters for the agricultural site and holds at about 1.1 down to three clusters where it drops to .81 . From this inspection it was concluded that four through eight clusters have about the same separability. The Qmin however is largest at four for this range. Thus if four through eight clusters are considered, four would be the optimum based on this data.

The average Q is higher for nine and ten clusters but the minimum is less than for four. From this data it was decided that four clusters optimally represented the agricultural site.

The urban site clustering demonstrated a relatively constant average Q of about 1.1 for ten down through six clusters. The Qmin peaked at .63 in this range for both seven and six clusters. This suggested six clusters for the urban site. The choice of number of clusters is partially subjective. Nine clusters gives a higher average of 1.14 and only a .01 reduction in Qmin. Eleven gives an average separation of 1.19 with the same minimum as six. Since we wish to find six clusters in the data and the $\overline{Q}$ for six is above unity with a local maxima for Qmin, six is chosen although no clear optimum exists. Next, the cluster maps were studied using topographic maps, aerial photography, and ground truth data to determine the contents of the clusters.

Examination of the four cluster map for the agricultural area revealed that three of the four multispectral change clusters (clusters 1,3,4) were largely corn fields. Cluster No. 2 tended to represent a no change condition. Table 9 contains the cluster mean changes and number of points in each cluster. Cluster one is the "brightest" cluster which is the usual case. The red band mean is 132.1 and since a 5.1 unit reduction in response is assumed to be due to the

Table 9 Estimated Changes in Cluster Means for the Agricultural Site for September 30 - October 19, 1973 Delta Data - Four Clusters, with Cluster 2 Assumed to be no change Cluster.

CLUSTER	NUMBER POINTS	CLUSTER MEAN CHANGES REFERENCED TO CLUSTER 2		
		MEAN FOR .6-.7 MICROMETER	MEAN FOR .7-.8 MICROMETER	MEAN FOR .8-1.1 MICROMETER
1	1025	+5.0	+6.3	+3.2
2	4213	0	0	0
3	4208	+2.6	-4.9	-3.6
4	655	+1.9	-16.2	-9.8

Table 10 Estimated Changes in Cluster Means for Urban Site over November 30, 1972 - June 9, 1973 Period. Six Clusters with Cluster 5 Assumed to be the No Change Cluster.

CLUSTER	NUMBER POINTS	CLUSTER MEAN CHANGES REFERENCED TO CLUSTER 5		
		BAND 2 .6-.7 MICROMETER	BAND 3 .7-.8 MICROMETER	BAND 4 .8-1.1 MICROMETER
1	823	+23.6	+17.1	+6.5
2	1979	+10.9	+5.1	+1.0
3	1934	-2.9	+14.2	+9.0
4	5008	-1.8	+6.1	+3.8
5	4175	0	0	0
6	622	-.9	-9.5	-7.1

Note: The discussion in the text of cluster mean changes for the agricultural site is based on a reference of 128.0 plus the assumed solar elevation effect whereas the numbers in Table 9 are referenced to the means of cluster 2. This represents two viewpoints for analyzing cluster mean changes.

lowered solar elevation, the actual change in the red values is estimated as +9.1 units. The means for the two infrared bands are 128.0 which implies an increase of 5.1 each. Thus, cluster one is assumed to represent green vegetation materials undergoing a general increase in reflectance probably due to yellowing and drying of the leaves and loss of the chlorophyll absorption in the red band. Cluster two includes grass, residential areas, shopping centers and is assumed to be the no change cluster. The red band mean is 127.0, the first IR band mean is 122.3 and the second IR band mean is 124.8 representing changes of +4.1, -.7, and +1.9 respectively. Cluster three includes the majority of corn fields in the site and many forest samples are also included. The change implied by the mean values for the red, IR one, and IR two bands is +6.7, -5.4, and -1.8 respectively. The physical process causing this change is assumed to be yellowing of leaves and initial deterioration of the cell structure of the leaves causing loss of the characteristic high infrared reflectance of green leaves. This is the second largest cluster with 41.6% of the total points and evidently represents a very widespread kind of change. Many forest samples and grass samples such as in the Purdue and Elks Country Club golf courses are included although in minor amounts. Cluster four is a small cluster (6.5% of the points) and contains corn fields which have undergone an unusually sharp decrease in

infrared reflectance. The estimated mean changes are +6.1, -16.7 and -8.0 for the red, IR-1, and IR-2 bands. These plants have lost reflectance in both IR bands whereas cluster three change was mostly in the .7 - .8 micrometers band (IR band 1). It was assumed these plants were in a more advanced stage of maturation. These interpretations are basically assumptions since no observations of the individual fields were made during the September 30 - October 19, 1972 period. Also, detailed discussion of the biophysical processes involved in reflectance of solar energy from plant leaves is beyond the scope of this paper. Thus, the conclusion drawn from the multispectral cluster analysis was that clusters 1, 3, and 4 represent corn plants in increasing stages of maturity with cluster 3 being the major change condition and including many non-corn changes and cluster 2 represents the no change condition. No appreciable change in soybean fields was indicated in this analysis.

The six cluster map for the urban site was inspected next for cluster content. The "bright" number 1 cluster contained bare soil areas mostly in the flatlands along the Wabash River. These are recently plowed areas in June 1973 which were covered with corn and soybean plants on September 30, 1972. The cluster mean changes are presented in Table 10, assuming cluster 5 is the no change cluster. The apparent

change in the red, IR-1 and IR-2 channels was +23.6, +17.1 and +6.5 respectively. Cluster two contained the majority of construction areas in the test site and is the cluster of greatest interest in this part of the study. The apparent changes in the three channels are +10.9, +5.1 and +1.0. Clusters 3 and 4 contained forest and heavily forested older residential areas. Cluster 5 contained downtown, water, industrial, and shopping center areas and was thus taken to be the no change cluster. Cluster six is a minor cluster and it is difficult to identify its contents. The mean changes for the three channels was -.9, -9.5 and -7.1. This cluster included areas such as the interchange on the Harrison Street Bridge and North River Road, a large portion of the Anheuser-Busch corn processing plant site, and areas of possible ponding. This cluster could not be definitively identified with regard to nature of change. These basic identifications were used as a basis for the supervised classification analysis which is described next.

Supervised Classification of Delta Images

The cluster maps for the agricultural and urban delta images were inspected for relationships between clusters and surface cover classification maps of Figures 10 and 11 as reference. In the agricultural area one of the predominately corn change clusters included many forest points so an

additional cluster was defined containing the forest points. This resulted in three corn change classes and two no change classes - one being the original no change cluster and the second the forest change cluster defined as no change. For the urban area test data the six cluster map was inspected and change categories assigned to each. One cluster showed a mixture of change sites and points where it was assumed no change took place so an additional class was defined for no change of interest to attempt to break it away from the construction change cluster. This cluster augmentation technique has previously proved useful in training the supervised classifier. Samples were chosen from each cluster for each site and used to train the supervised classifier. Classification was performed on the agricultural and urban sites and the training field results are presented in Tables 11 and 12. The classification maps are presented in Figure 14 for the agricultural area and Figure 15 for the urban area.

Results of Crop Change Detection Experiment

The change classification map (Figure 14) for the agricultural site was regenerated using the symbol + for the 3 corn change classes and the two remaining classes were left blank. The corn change only classification map is presented in Figure 16. Inspection of the location of the corn change points showed that the majority did fall within corn fields.

Table 11 Training Sample Results for Supervised Change Classification of the Agricultural Test Site.

CLASS	NUMBER POINTS	PERCENT CORRECT	TYPICAL SURFACE COVER
CORN1	41	97.6	Twenty to forty acre corn fields
CORN2	61	86.9	Twenty to forty acre corn fields
CORN3	28	100.0	Twenty to forty acre corn fields
No Change	153	76.5	Soybeans & Commercial Areas
Tree Change	25	76.0	Dense twenty acre woods
Overall	308	83.4	

Table 12 Training Sample Results for Supervised Change Classification of Urban Test Site.

CLASS	NUMBER SAMPLES	PERCENT CORRECT	TYPICAL SURFACE FEATURE IN CLASS
Bare Soil	24	95.8	Plowed corn fields
Construction	14	71.4	Shopping & Housing Projects
No Change of Interest	51	56.9	Gravel pits
Forest Change	24	95.8	Mixed forest
Residential Change	40	95.0	Older forested residences
No Change	35	100.0	Downtown Lafayette
Unknown	18	94.4	---
Overall	206	85.0	

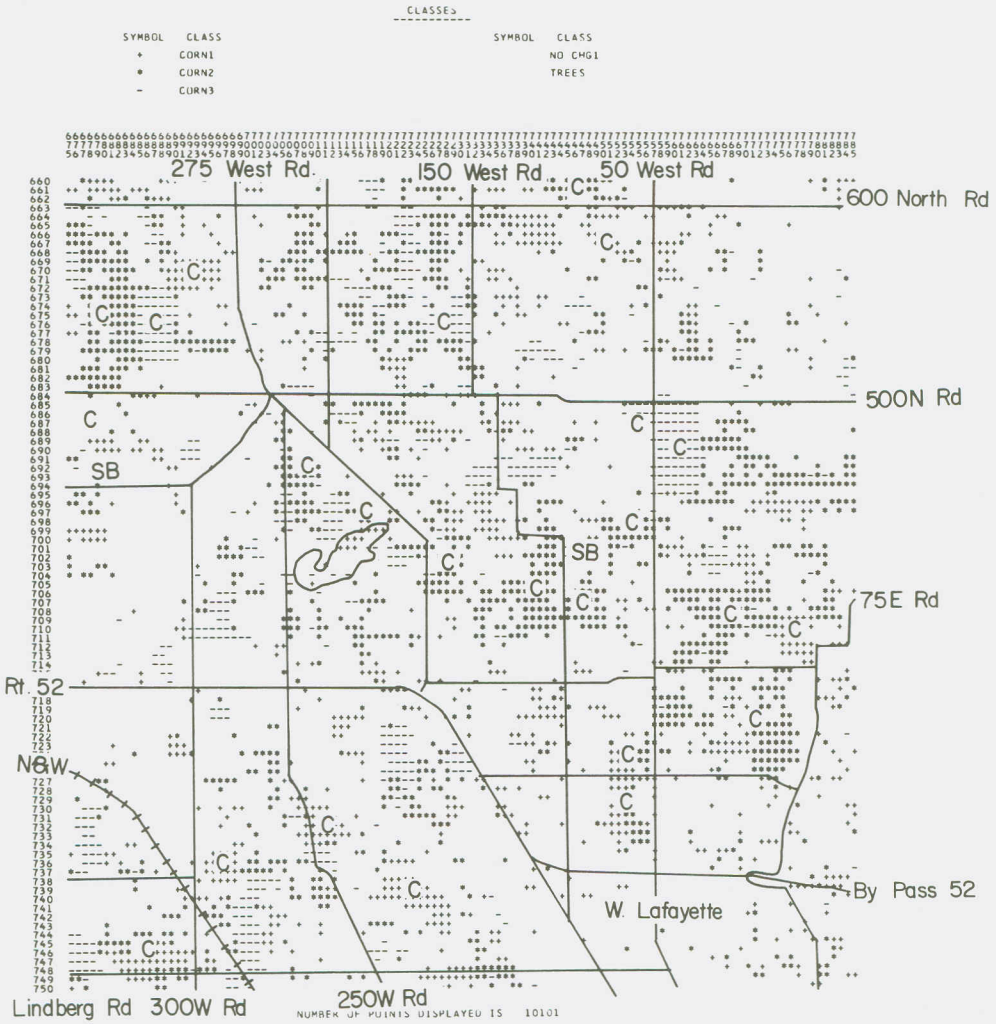

Figure 14. Supervised change classification printout of agricultural test site with three categories of change in corn fields indicated. All four October 19 delta spectral bands were used. Ground truth symbols, C for corn and SB for soybeans, are included for certain fields. Points classified as no change are printed as blanks.

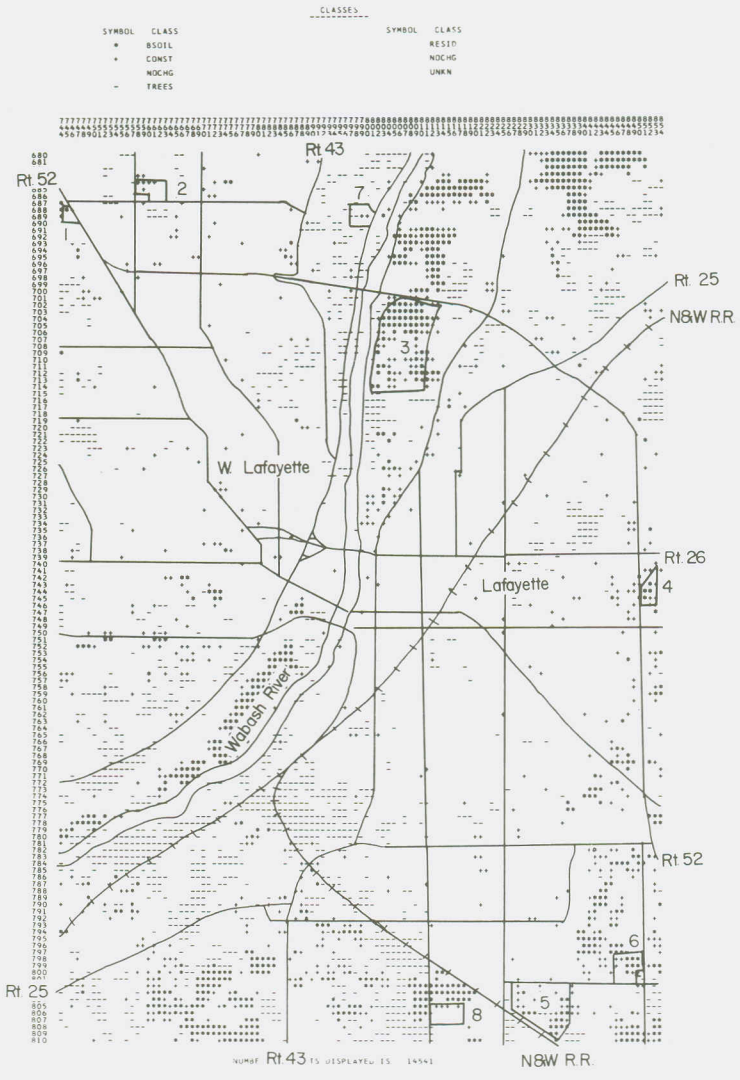

Figure 15. Supervised change classification for the urban test site with three categories of change shown. All four June 9, 1973 delta spectral bands were used. The construction change class points are printed as + signs. No change points are blank.

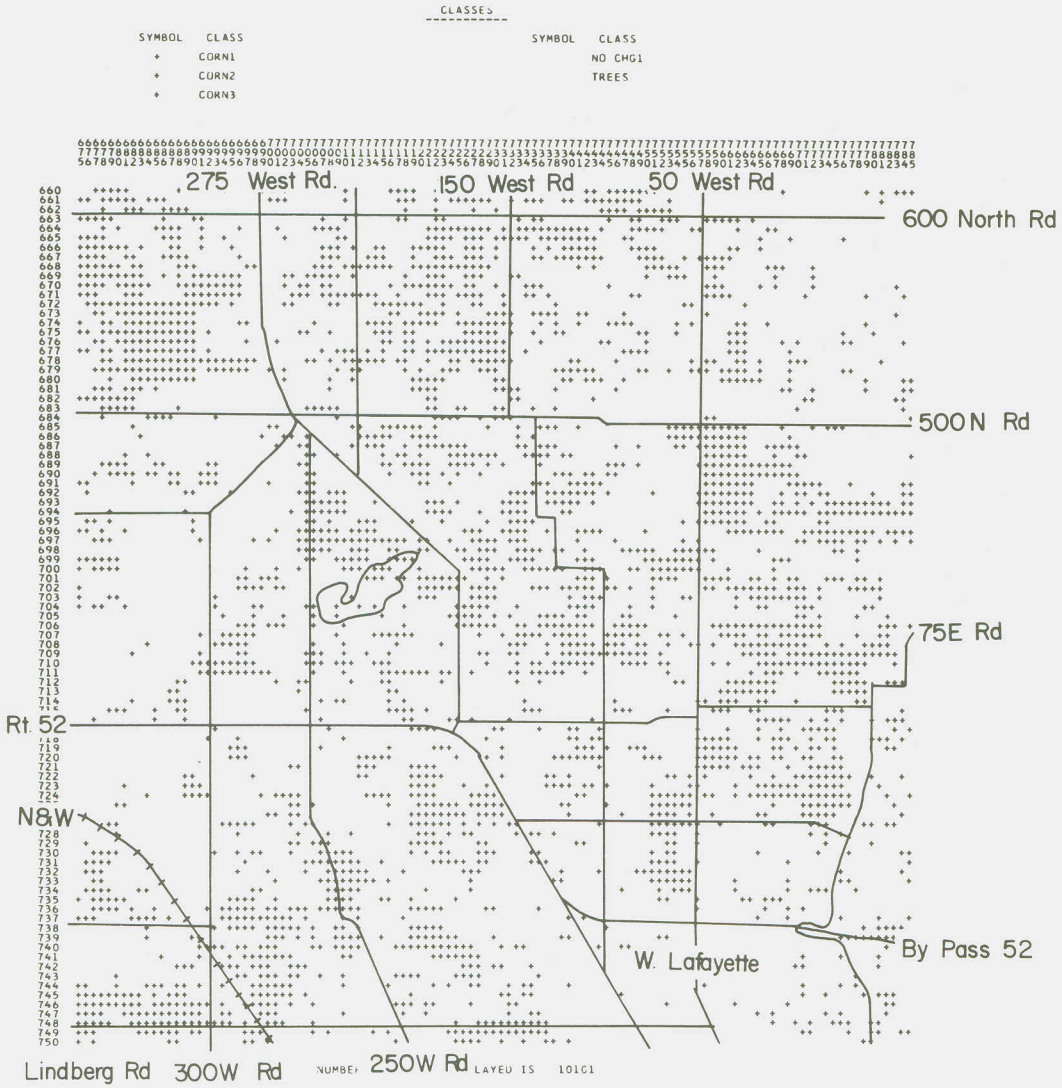

Figure 16. Agricultural site change classification with all three categories of corn change printed as a + sign. All other details same as Figure 14.

A large number were seen outside known or inferred corn fields however. A detailed evaluation was carried out manually by inspecting each change point and observing whether or not it fell in a reference corn field. In the 10,101 point test site 3,183 points were classified as corn change and 6,918 were classified as change of no interest or no change at all. Of the 3,183 corn change points 2,168 fell inside reference corn fields. The total number of corn points estimated from the classification in Figure 10 augmented with additional ground truth and aerial photography information was 2,997. Since 2,168 of the 3,183 corn change points coincided with certain of the 2,997 corn points the corn change detection accuracy is taken as 68%.

If conditional change detection classification were performed only the fields known to contain the material of interest would be change classified and the evaluation of change would be potentially much more accurate. Further inspection of the change map indicates that most of or all of a particular field changes if a change does occur. Therefore isolated change points could be ignored. The stated accuracy of 68% is thus a very preliminary result.

Results of Urban Change Detection Experiment

Inspection of the seven change class map in Figure 15 for the urban site reveals remarkably good agreement between

known surface change conditions and the three change classes printed: Bare soil (*), construction (+) and trees (-). The bare soil change class arises from surfaces which were covered with crops or grass and weeds on September 30, 1972 and were plowed soil or bare soil due to construction on June 9, 1973. Most of this class consisted of plowed agricultural fields such as the area along the Wabash River around line 760 and column 775 and in the Northeast corner of the area. Four construction related bare soil indications were observed. The largest is at construction site 3 where a city golf course is under development. Weeds and grass existed there in September 1972 and the area was mostly graded bare soil in June 1973. The second example is at site 1 where ground was cleared for a motel during the period. A similar situation exists at site 4 where a shopping center parking lot was under construction and at site 5 where a housing addition was expanding.

The construction change class relates more to points that have changed from grass and weeds to a mixture of construction-related surface covers including concrete, bare soil, roof tops, grass, gravel and macadam. All the construction sites demonstrated some of this class. Figure 17 contains the classification map with only the construction class printed with plus signs. One construction class point was observed at site 1 where some building superstructure was up.

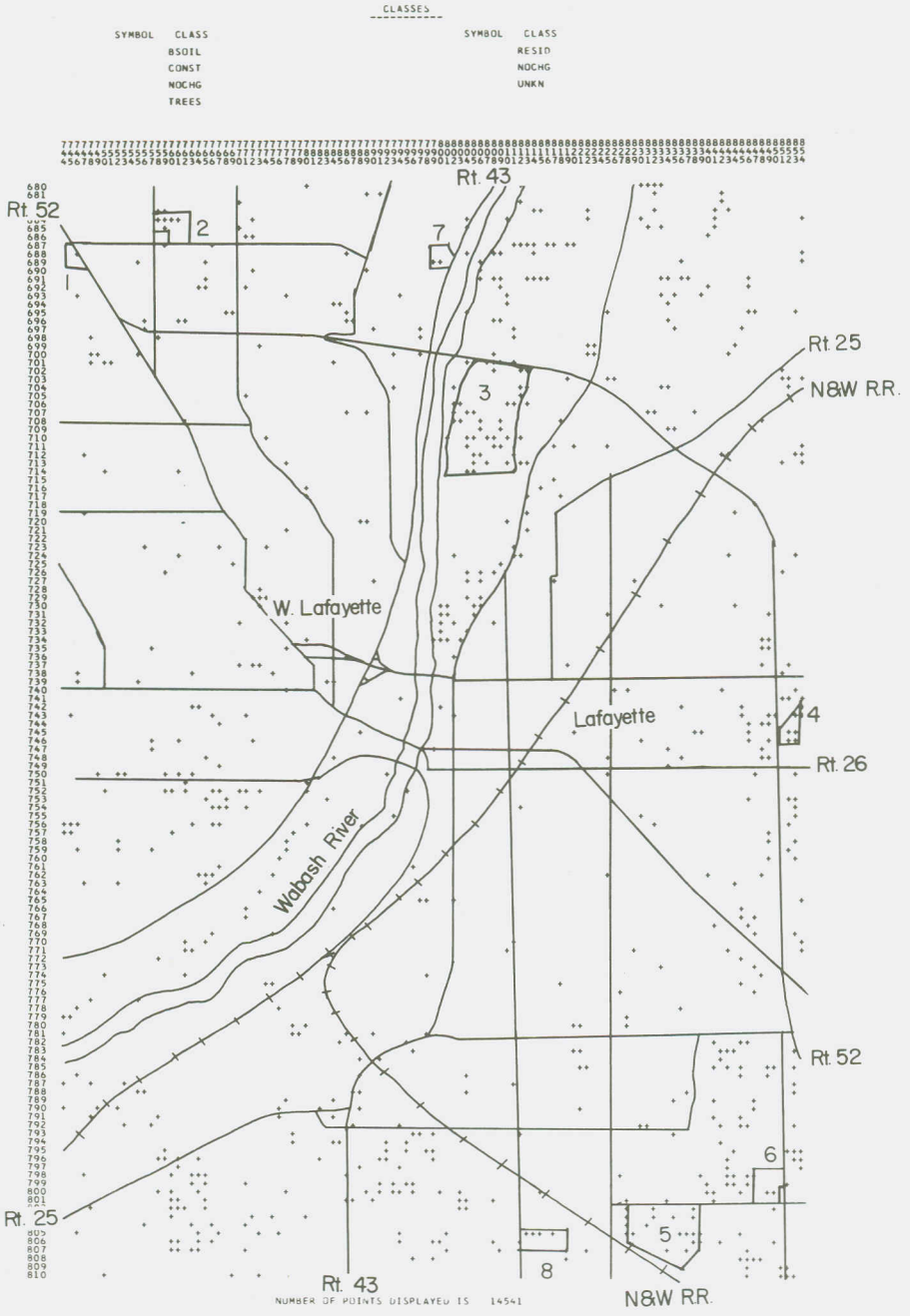

Figure 17. Urban site change classification with construction change classifications printed as + signs and all other classes printed as blank. All other details same as Figure 15.

At site 2 a cluster of apartment buildings were on the site by June 9 and this site was totally classified as construction. Site 3 showed very little construction classifications since it is a golf course and no building or paving materials were brought on the site. The shopping center building on the back of site 4 was correctly classified as construction. Site 5 consists of a row of new condominiums of the West edge and housing construction elsewhere. A row of 5 pluses over the line of the condominiums indicated correct classification there. A row of new houses in site 8 was correctly identified and construction of an addition to a sanitarium at site 7 was related to two construction class pixels at that location. The tree change points fell over areas of heavy forestation mostly along the West bank of the Wabash River North of the city and South of the city along the East bank. These changes are assumed to be due to differences in stage of leaf growth and Fall coloration.

Unfortunately a large number of construction change points were generated where no construction existed and this large "false alarm" error rate will require further study to define classification techniques to suppress these errors. A visual check of the 754 construction change points in Figure 17 indicated that about 120 might be associated with construction, about 150 were in areas of gravel (mostly limestone gravel

parking lots), about 250 were in corn and soybean fields, 50 were in grassy areas and the remainder could not be identified with the information available. It was concluded that due to the heavy rains in the area in the evening of November 28 when 1.62 inches of rain fell and the generally very wet condition of the soil due to heavy rain throughout September (9 inches from September 1 thru September 30, 1972) the change classification results were not typical of what could ultimately be achieved. The good agreement of construction classification points with observed construction activity indicates that the method has promise but further work must be done to test and develop it using data from times when environmental conditions are similar. Presumably a 12 month interval would be best for construction change detection since all vegetative cover would be in very similar state at similar times in the growing season. Also, times when the soil and scene in general is on about the same state of dryness should be selected to avoid the problems due to rainfall differences encountered in this investigation.

V Summary and Conclusions

An analysis of the use of the temporal dimension for crop species classification and urban change detection is presented. ERTS-1 multispectral scanner data from several times between August 1972 and June 9, 1973 were digitally registered and analyzed, using multispectral pattern recognition techniques.

In the crop species identification experiment the classes corn, soybeans and "other" were classified using multispectral data from one, two, and three times in various combinations. Results indicate that using spectral channels from different times can improve classification accuracy for certain times of the growing season but not for other time combinations. In the experiment here results for August 9 data only were better than for any combination of August 9, September 19 and October 2 spectral channels. However, use of September 19 and October 2 channels together produced a significant improvement in classification accuracy (11,5%) over that obtained with either September or October channels alone. This result suggests strongly that temporal data can be of significant benefit in crop species classification in certain cases.

In the change detection experiment multispectral pattern recognition techniques were applied to difference data

obtained by subtracting a reference multispectral image from another multispectral image obtained at a later time. Four categories of change were identified in an agricultural scene and seven classes of change were identified in an urban scene. Three of the four categories of agricultural change were related to change in corn fields over a 19 day period. Quantitative evaluation indicated that 68% of the corn change points actually fell in corn fields. One of the categories of urban change related to construction changes and eight ground truthed construction sites were correctly classified. However, a large number of construction classification points fell in areas where no construction existed. The method shows promise for automatic identification of urban change but further work is required to reduce the "false alarm" rate for change classification.

The concept of an information functional was introduced to focus attention on the general type of transformation being performed on the remote sensor data. An information functional maps a radiometric measurement function of wavelength, $f(\lambda)$, or in the present study a function of wavelength and time $f(\lambda,t)$ into a number representing some information measure. In the study discussed here the information functional is of the form $C=L(f(\lambda,t),P)$ where C is a class index representing corn, soybeans, construction change,

no change etc., L is the transformation process and P is a set of parameters defining the particular transformation. The form of L in the present study is a Gaussian maximum likelihood classifier.

This report describes specific techniques for analyzing temporal data for crop classification and change detection. Many other possible techniques exist and should be investigated. The results obtained from one crop classification experiment and one urban change detection experiment suggest that these techniques have potential but further work is required to determine if error rates can be reduced to acceptable levels. The Gaussian assumption was not tested for the change detection classification since the training sample sizes were extremely small. A thorough analysis of the statistics of the temporal data should be conducted so that an optimum classification process can be defined.

References

1. K. S. Fu, D. A. Landgrebe, T. L. Phillips, "Information Processing of Remotely Sensed Agricultural Data", Proceedings of the IEEE, Vol. 57, pp. 639-653, April 1969.

2. H. W. Smedes, M. M. Spencer, F. J. Thomson, "Processing of Multispectral Data and Simulation of ERTS Data Channels to make Computer Terrain Maps of Yellowstone National Park Test Site", Third Annual Earth Resources Program Review (NASA - MSC, Houston, Texas), December 1970.

3. R. E. Marshall, N. S. Thomson, F. J. Kriegler, "Use of Multispectral Recognition Techniques for Conducting Wide Area Wheat Surveys", Proc. 6th. International Symposium on Remote Sensing of Environment, University of Michigan, Ann Arbor, Michigan, pp. 3-20, 1969.

4. M. G. Tanguay, R. M. Hoffer, R. D. Miles, "Multispectral Imagery and Automatic Classification of Spectral Response for Detailed Engineering Soils Mapping", Proc. 6th. International Symposium on Remote Sensing of Environment, (Ann Arbor, Michigan), pp. 33-64, 1969.

5. G. C. Cheng, R. S. Ledley, D. K. Pollock, A. Rosenfeld, "Pictorial Pattern Recognition", Thompson Book Company, Washington, D. C., 1968.

6. R. L. Lillestrand, "Techniques for Change Detection", IEEE Transactions on Computers, Vol. C-21, No. 7, July 1972.

7. C. F. Lam, R. R. Hoyt, "High Speed Image Correlation for Change Detection", presented at National Aeronautics and Electronics Conference (NAECON), Dayton, Ohio, May 15 - 17, 1972.

8. D. Steiner, "Time Dimension for Crop Surveys from Space", Photogrammetric Engineering, Vol. 36, pp. 187-194, 1970.

9. P. E. Anuta, "Spatial Registration of Multispectral and Multitemporal Digital Imagery Using Fast Fourier Transform Techniques", IEEE Transactions on Geoscience Electronics, Vol. GE-8, pp. 353-368, October 1970.

10. ERTS Data Users Handbook, Document No. 7154249, Goddard Space Flight Center, NASA, Greenbelt, Maryland, 1972.

11. IBM 4507 Digital Image Display System Operations Manual, IBM Federal Systems Division, Gaithersburg, Maryland, October, 1970.

12. P. E. Anuta, "Geometric Correction of ERTS-1 Digital Multispectral Scanner Data", LARS Information Note 103073, Laboratory for Applications of Remote Sensing, 1220 Potter Drive, West Lafayette, Indiana, October 1973.

13. P. H. Swain, "Pattern Recognition: A Basis for Remote Sensing Data Analysis", LARS Information Note 111572, Laboratory for Applications of Remote Sensing, 1220 Potter Drive, West Lafayette, Indiana, November 1972.

14. A. G. Wacker, D. A. Landgrebe, "Boundaries in Multispectral Imagery by Clustering", 1970 IEEE Symposium on Adaptive Processes, Decision and Control (9th), pp. X14.1 - X14.8, December 1970.

15. P. J. Min, K. S. Fu, "On Feature Selection in Multiclass Pattern Recognition", School of Electrical Engineering, Purdue University, West Lafayette, Indiana, Technical Report TR-EE68-17, July 1968.

16. J. G. Kawamura, "Automatic Recognition of Changes in Urban Development from Aerial Photographs", IEEE Transactions on Systems, Man and Cybernetics, Vol. SMC-1, No. 3, pp. 230-239, July 1971.

17. M. E. Bauer, J. E. Cipra, "Identification of Agricultural Crops by Computer Processing of ERTS MSS Data", Proceedings of Symposium on Significant Results Obtained from ERTS-1. March 5-9, 1973, pp. 205-212, New Carrollton, Maryland.